Supporting Information for

Water-Soluble Phosphaviologens for Effective Photo-Induced Charge Separation

*Monika Stolar, Belinda Heyne, and Thomas Baumgartner**

Department of Chemistry & Centre for Advanced Solar Materials, University of Calgary,
2500 University Drive N.W.
Calgary, Alberta, Canada, T2N 1N4
e-mail: Thomas.baumgartner@ucalgary.ca

Contents

General Procedures and Equipment. Reactions were carried out under ambient conditions unless otherwise specified. 4-(Bromomethyl)benzoic acid, methyl 4-(bromomethyl)benzoate, and methyl triflate were purchased from Sigma Aldrich; TiO_2 (anatase, 10 nm, Photocatalyst) was purchased from MKnano division of M K Impex Corp. and used without further purification. N-Methyl-4,4'-bipyridinium iodide,[S1] 2,7-diazadibenzophosphole oxide,[S2] N-methyl-2,7-diazadibenzophosphole oxide triflate[S3] were prepared according to previously reported literature procedures. Microwave synthesis was carried out in a CEM Discover microwave. NMR solvents were purchased from Sigma Aldrich. $^{31}P\{^1H\}$ NMR, ^1H NMR, $^{19}F\{^1H\}$ NMR, and $^{13}C\{^1H\}$ NMR were recorded on Bruker Avance (-II,-III) 400 MHz spectrometers. Chemical shifts were referenced to external 85% H_3PO_4 (^{31}P), C_6F_6 (^{19}F) and external TMS (^1H, ^{13}C) or residual non-deuterated solvent peaks (^1H, ^{13}C). Mass spectra were run on a Finnigan SSQ 7000 spectrometer or a Bruker Daltonics AutoFlex III system. Elemental analyses were performed in the Department of Chemistry at the University of Calgary. Thermogravimetric Analysis (TGA) was performed on a TA-Instruments Q50 instrument. Cyclic voltammetry analyses were performed on an Autolab PGSTAT302 instrument, with a polished glassy carbon electrode as the working electrode, a Pt-wire as counter electrode, and an Ag wire as reference electrode, using ferrocene/ferrocenium (Fc/Fc^+) as internal standard. If not otherwise noted, cyclic voltammetry (CV) experiments were performed in acetonitrile solution with tetrabutylammonium hexafluorophosphate (0.1M) as supporting electrolyte. Zeta potentials were measured using a Malvern Zetasizer ZS. UV-vis experiments were carried out in water and methanol/ethanol on a UV−Vis−NIR Cary 5000 spectrophotometer and UV-Vis Cary 50. Crystal data and details of the data collection are provided in Table S2. Irradiation was performed with a 2W LED purchased from Lumex, whose spectral profile can be found in Figure S40. Diffraction data were collected on a Bruker SMART CCD X-ray Diffractometer. CCDC 1526886 contains the supplementary crystallographic data for this paper. These data can be obtained free of charge from The Cambridge Crystallographic Data Centre via www.ccdc.cam.ac.uk/data_request/cif.

Conditioning of TiO_2. The commercially available TiO_2(anatase), was dried overnight under vacuum at 120 °C, then purged with N_2 and kept under inert atmosphere until used.

TiO_2 Functionlization with MVA. The dried TiO_2 nanoparticles were functionalized using a 1.2 wt% dispersion in a methanol solution containing **MVA** (2.6 x 10^{-2} M). The mixture was ultrasonicated for 30 min or 2 hrs at room temperature followed by centrifugation of the dispersion to isolate the functionalized nanoparticles (**TiO_2MVA**) yielding 4.8% **MVA** loading.

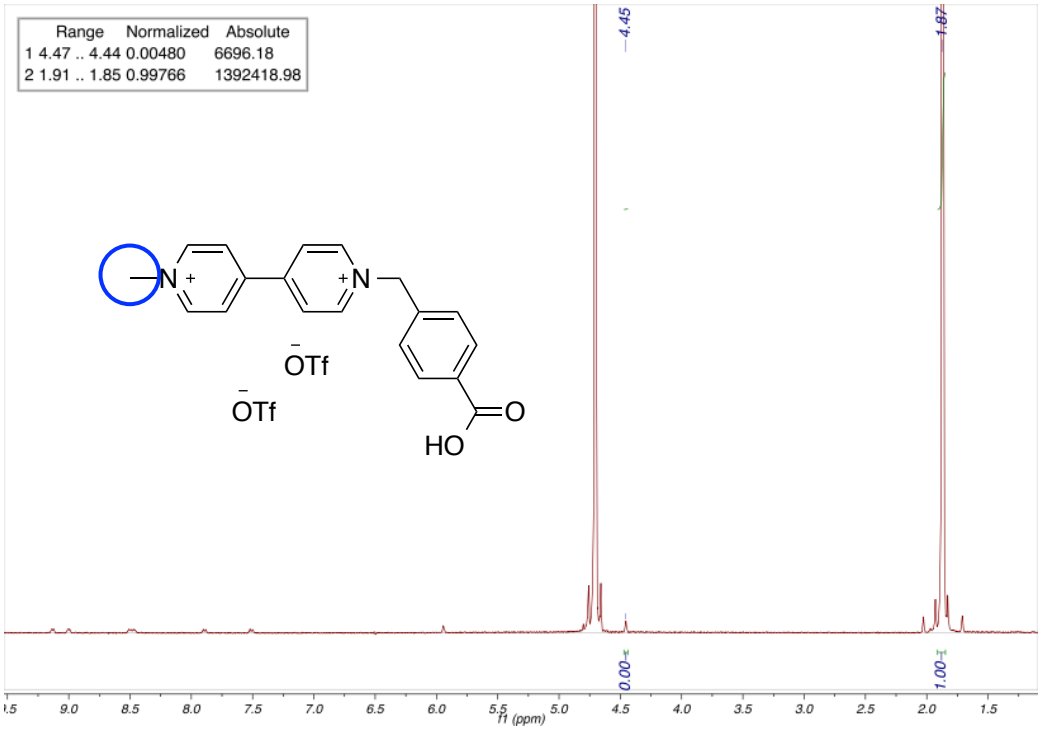

Figure S1. ^{1}H NMR of washed TiO_2MVA in 0.035 M sodium acetate in D_2O (circled protons show those used for integration).

Loading Calculation

$$0.035\ mmol\ (\text{sodium acetate})\ x\ \frac{0.0048\ (\text{MVA})}{0.99766\ (\text{sodium acetate})}$$

$$= 0.00016839\ mmol\ (\text{MVA})$$

$$0.00016839\ mmol\ x\ 604.49\frac{g}{mol} = 0.10179251\ mg\ (\text{MVA})$$

$$\frac{0.10179251\ mg\ (\text{MVA})}{2.1\ mg\ (\text{TiO2MVA})}\ x\ 100\ \% = 4.8\ \%$$

TiO_2 Functionalization with PVA. The dried nanoparticles were functionalized using a 1.3 wt% dispersion in a methanol solution containing **PVA** (2.6 x 10^{-2} M). The mixture was ultrasonicated for 30 min or 2 hrs at room temperature followed by centrifugation of the dispersion to isolate the functionalized nanoparticles (**TiO_2PVA**) yielding 2.9% **PVA** loading.

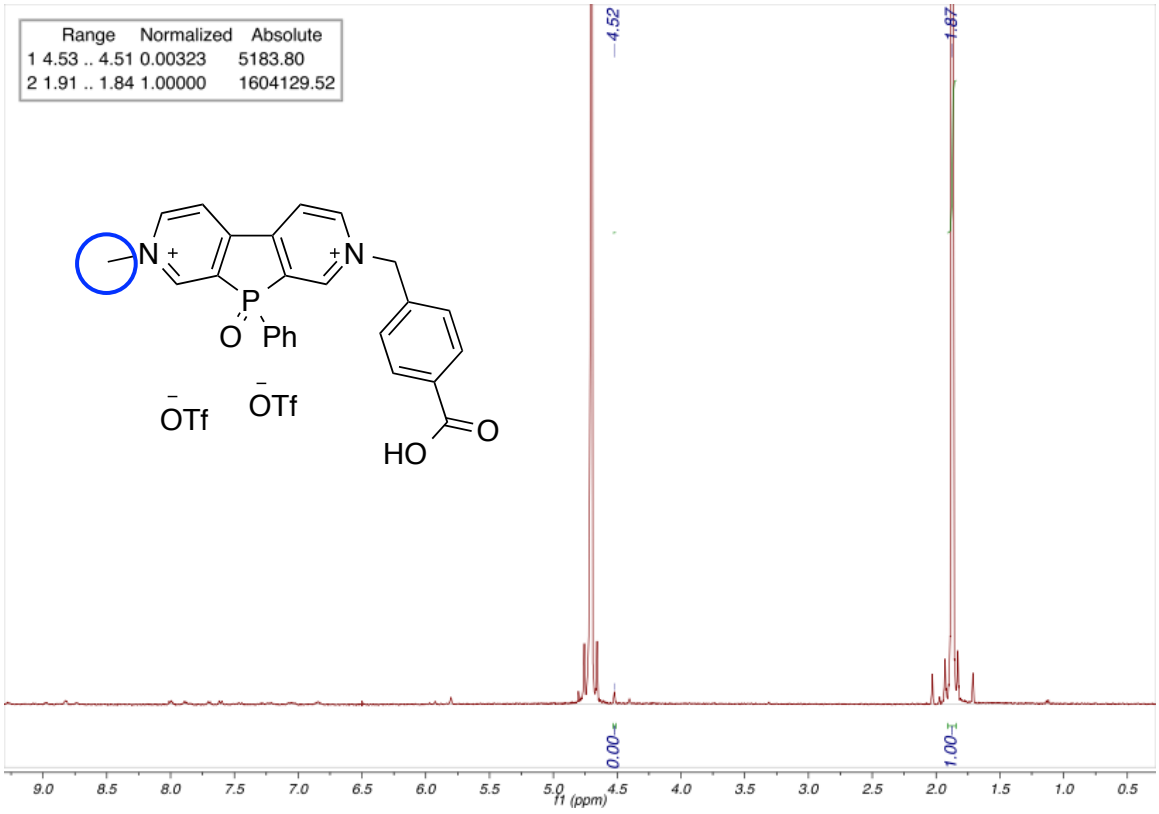

Figure S2. ^{1}H NMR of washed TiO_2PVA in 0.035 M sodium acetate in D_2O (circled protons show those used for integration).

Loading Calculation

$$0.035\ mmol\ (\text{sodium acetate})\ x\ \frac{0.00323\ (\text{PVA})}{1.00000\ (\text{sodium acetate})}$$

$$= 0.00011305\ mmol\ (\text{PVA})$$

$$0.00011305\ mmol\ x\ 726.55\frac{g}{mol} = 0.08213648\ mg\ (\text{PVA})$$

$$\frac{0.08213648\ mg\ (\text{PVA})}{2.8\ mg\ (\text{TiO2PVA})}x\ 100\ \% = 2.9\ \%$$

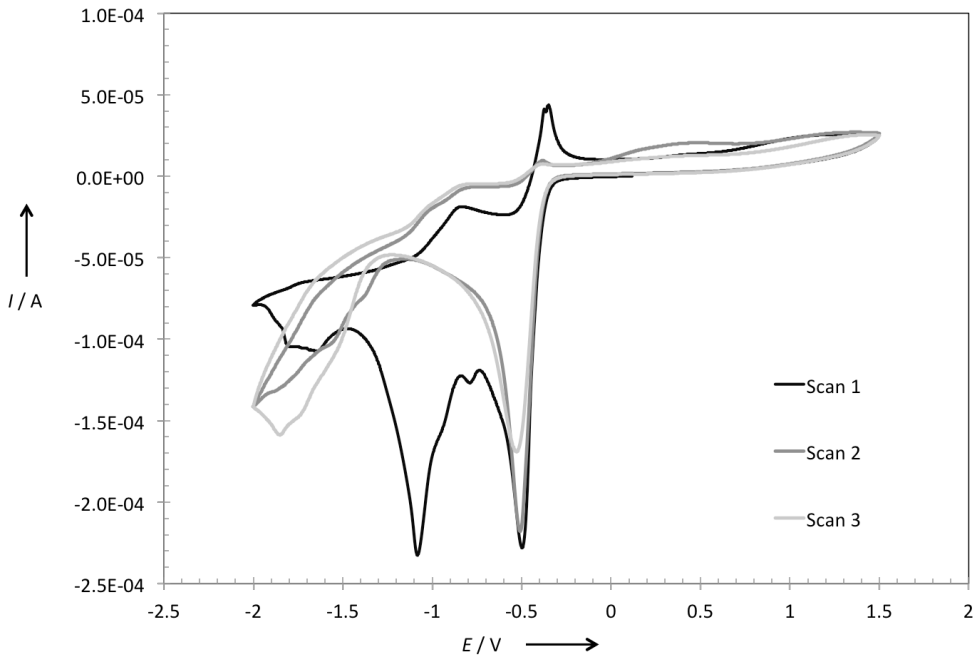

Figure S3. Electrochemistry of MVA. Cyclic voltammogram of **MVA** in acetonitrile solution with tetrabutylammonium hexafluorophosphate (0.1M) as supporting electrolyte after multiple scans showing irreversible build up of material on electrode.

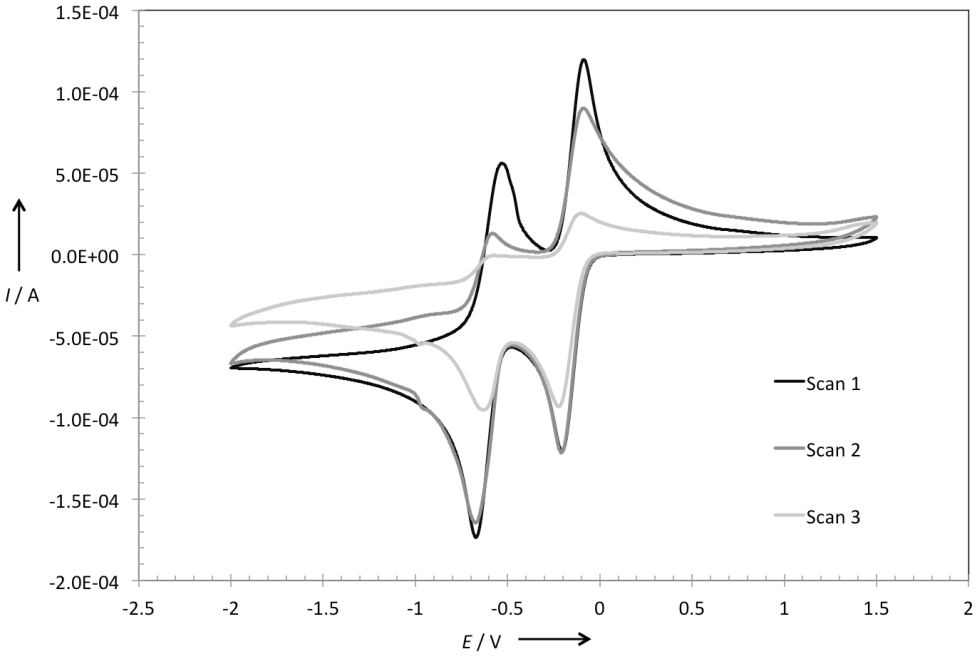

Figure S4. Electrochemistry of PVA. Cyclic voltammogram of **PVA** in acetonitrile solution with tetrabutylammonium hexafluorophosphate (0.1M) as supporting electrolyte after multiple scans showing irreversible build up of material on electrode.

Table S1. CV data for **MVA** and **PVA** in acetonitrile solution with tetrabutylammonium hexafluorophosphate (0.1M) as supporting electrolyte

Compound	$E_{red1,cathodic\ peak}$	$E_{red2,cathodic\ peak}$
MVA	-0.49 V	-1.08 V
PVA	-0.20 V	-0.67 V

Due to the poor behavior of these species under the specified condition the cathodic peaks are reported without the use of an internal reference and are referenced to an Ag/Ag^+ wire.

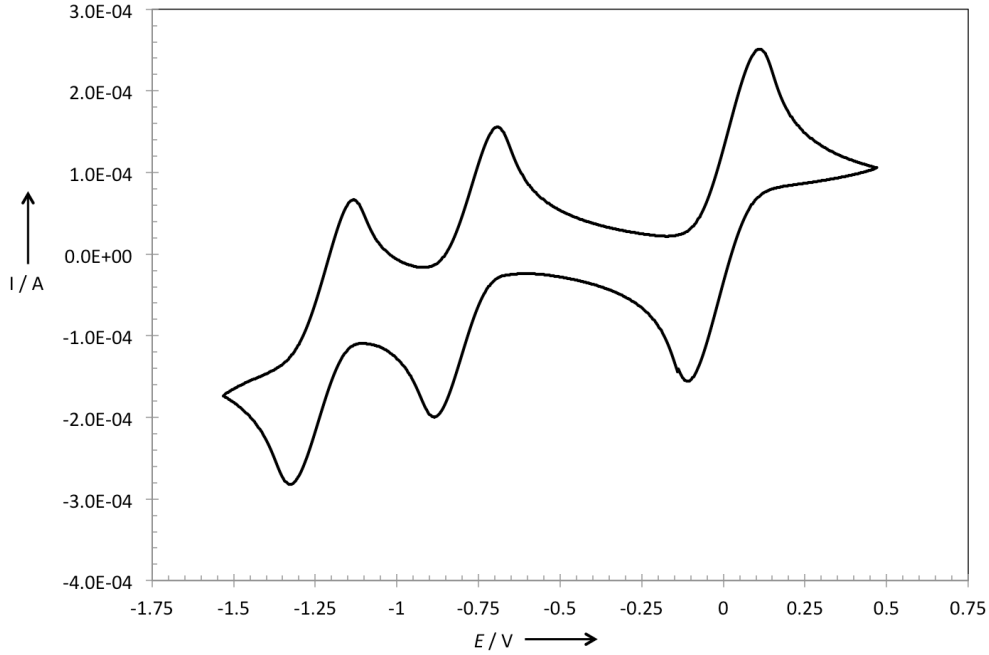

Figure S5. Electrochemistry of MVE. Cyclic voltammogram of **MVE** in acetonitrile solution with tetrabutylammonium hexafluorophosphate (0.1M) as supporting electrolyte, potential E referenced to Fc/Fc^+ as an internal standard.

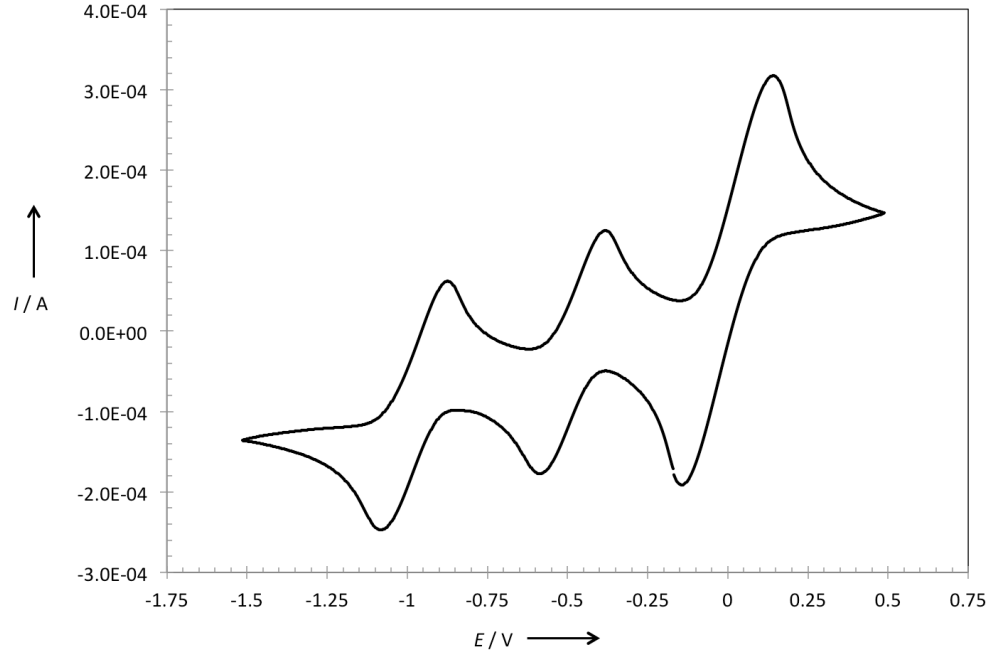

Figure S6. Electrochemistry of PVE. Cyclic voltammogram of **PVE** in acetonitrile solution with tetrabutylammonium hexafluorophosphate (0.1M) as supporting electrolyte, potential E referenced to Fc/Fc^+ as an internal standard.

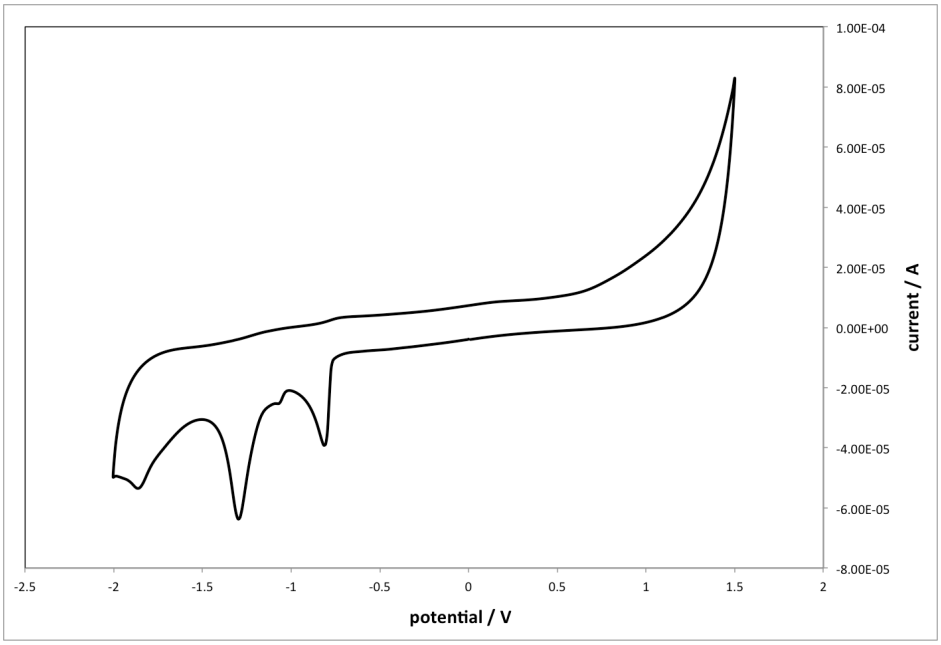

Figure S7. Electrochemistry of MVA. Cyclic voltammogram of **MVA** in water with lithium perchlorate (0.1M) as supporting electrolyte.

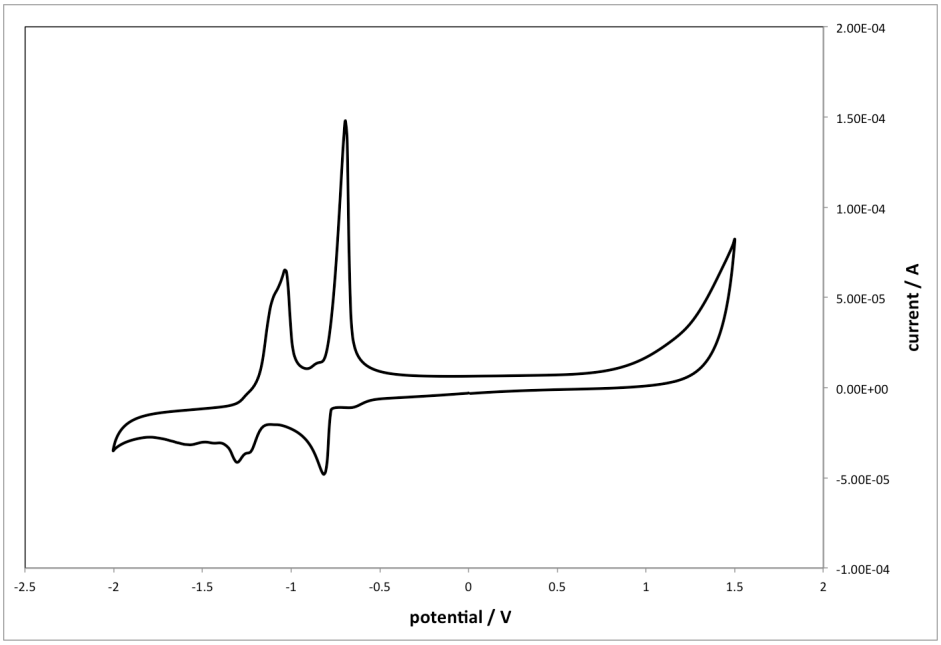

Figure S8. Electrochemistry of MVE. Cyclic voltammogram of **MVE** in water with lithium perchlorate (0.1M) as supporting electrolyte.

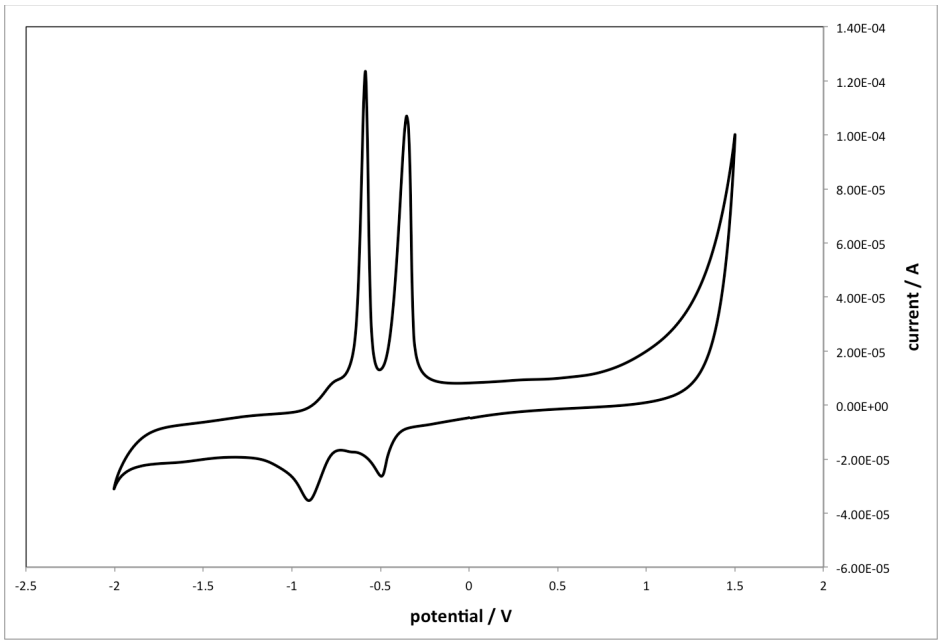

Figure S9. Electrochemistry of PVA. Cyclic voltammogram of **PVA** in water with lithium perchlorate (0.1M) as supporting electrolyte.

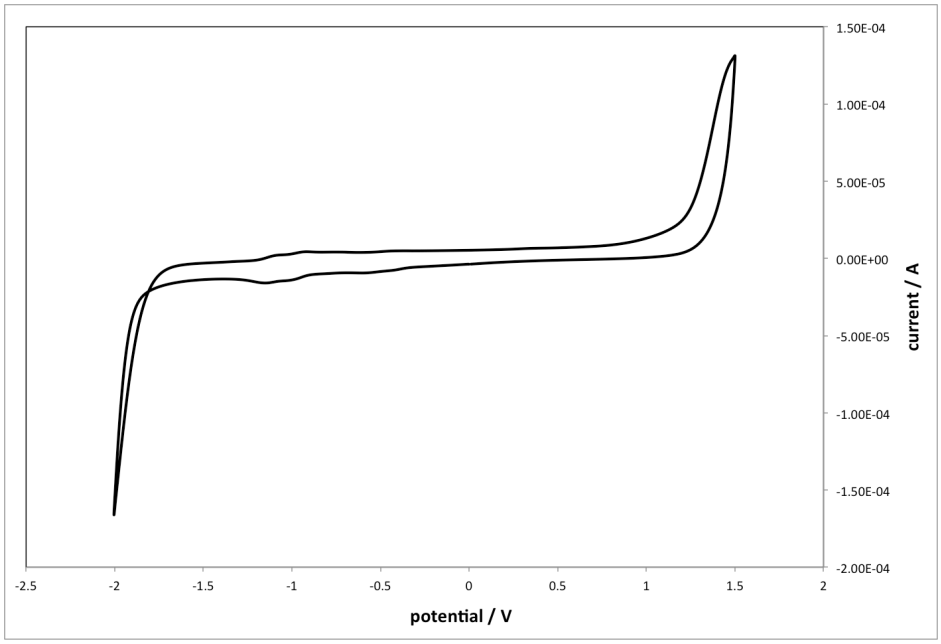

Figure S10. Electrochemistry of PVE. Cyclic voltammogram of **PVE** in water with lithium perchlorate (0.1M) as supporting electrolyte.

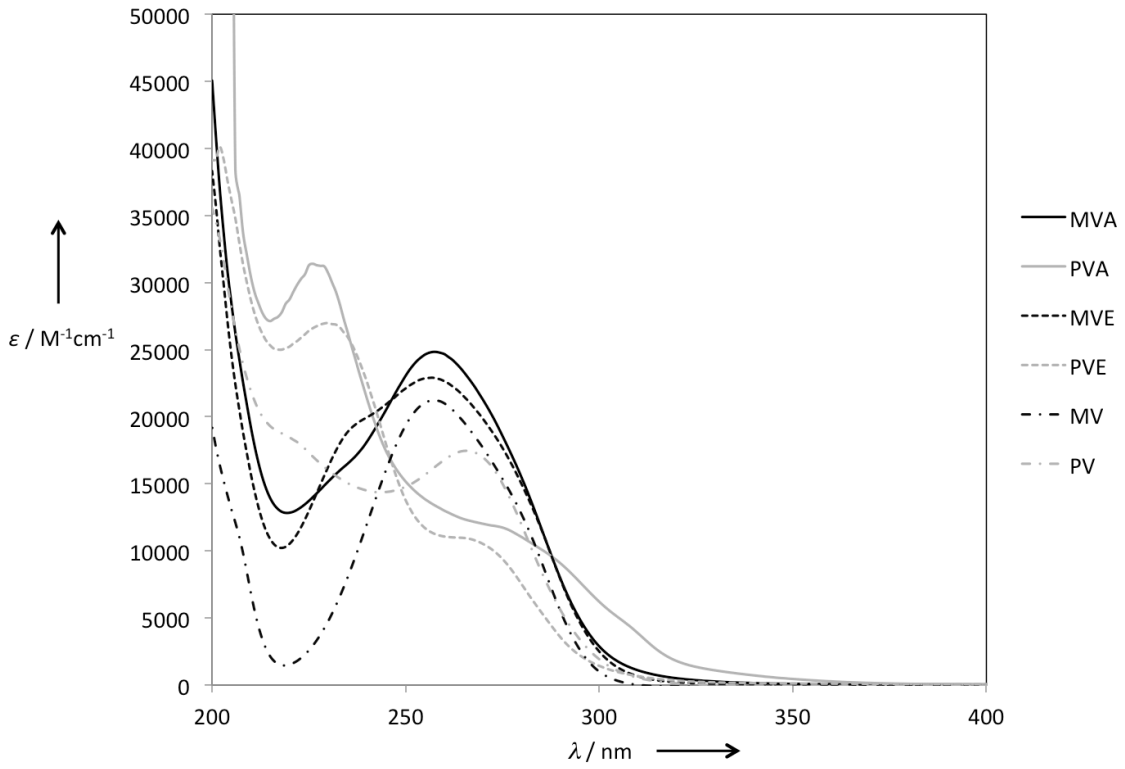

Figure S11. UV-Vis of diquaternized salts. UV-Vis spectra of the synthesized dicationic salt species (no features at 400-800 nm) in deionized water.

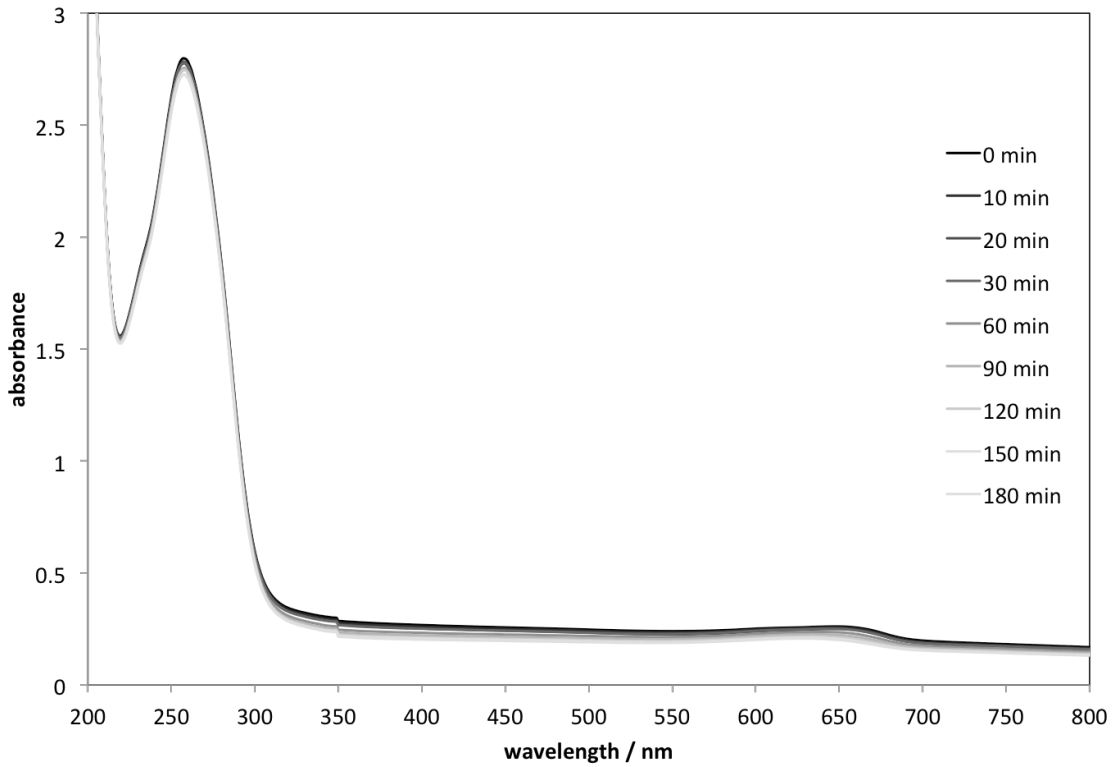

Figure S12. Evolution of the absorption spectrum of **MVA** under aerobic irradiation at 406 nm in water in the presence of **TiO_2**.

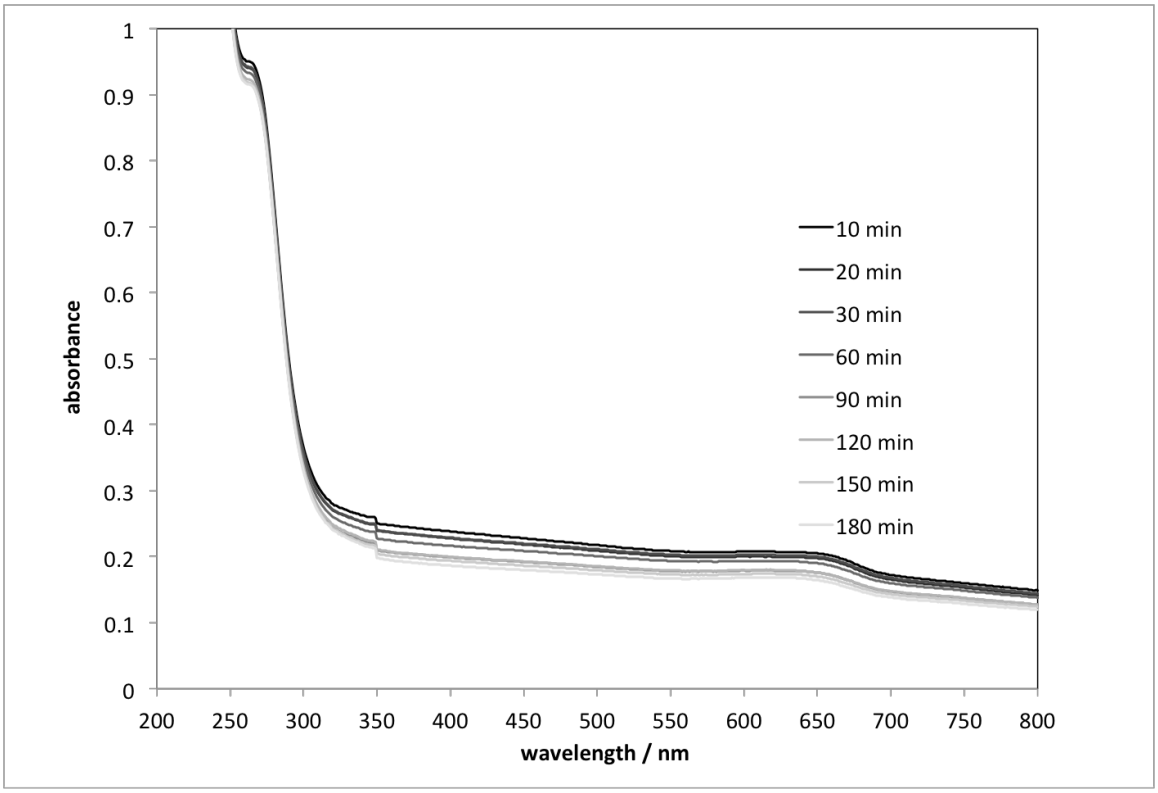

Figure S13. Evolution of the absorption spectrum of **PVA** under aerobic irradiation at 406 nm in water in the presence of $\mathbf{TiO_2}$.

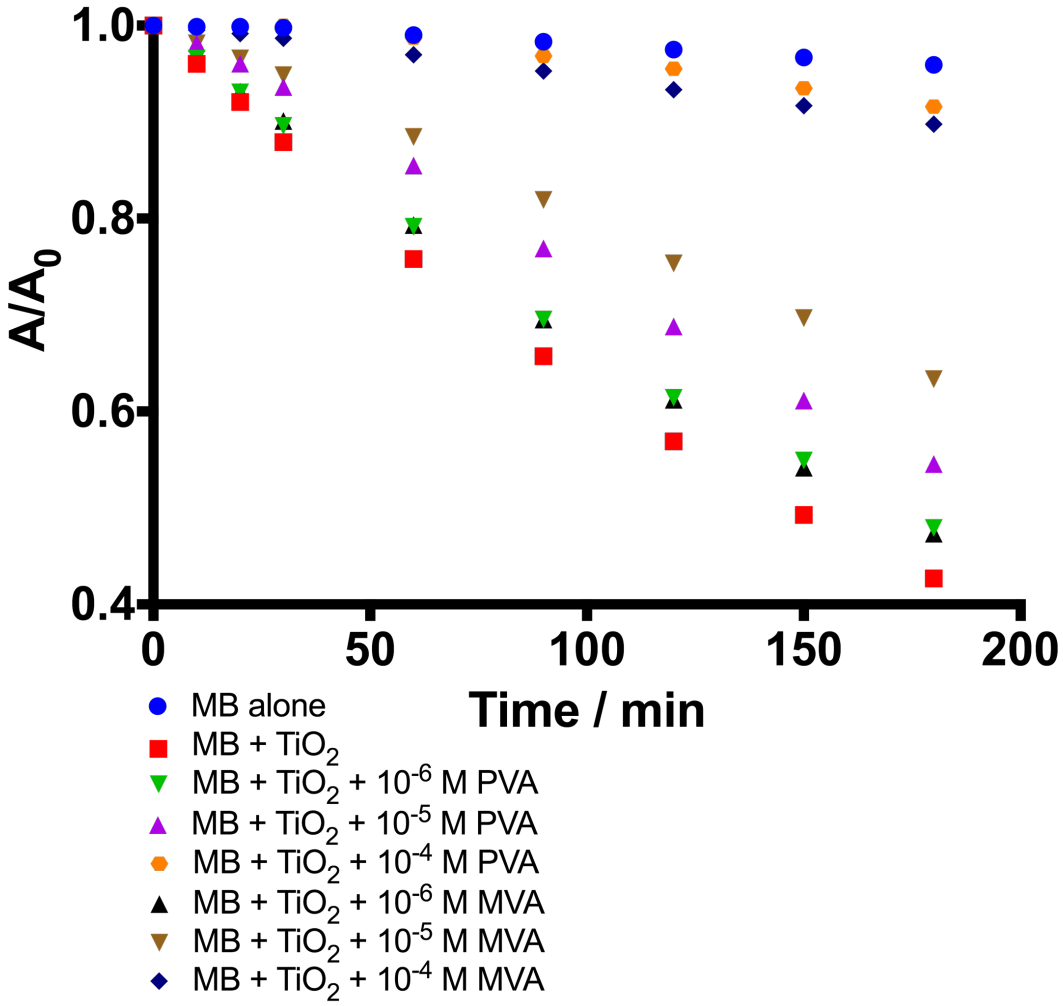

Figure S14. Comparison of methylene blue photodegradation kinetics with all species tested.

Table S2. Crystal data and structure refinement for **MVA**.

Identification code	BZAMVOTF	
Empirical formula	$C_{21}\ H_{18}\ F_6\ N_2\ O_8\ S_2$	
Formula weight	604.49	
Temperature	173(2) K	
Wavelength	1.54178 Å	
Crystal system	Triclinic	
Space group	P-1	
Unit cell dimensions	a = 8.67730(10) Å	α = 101.7870(10)°.
	b = 16.4779(2) Å	β = 91.1760(10)°.
	c = 26.3132(3) Å	γ = 92.2310(10)°.
Volume	3678.67(8) $Å^3$	
Z	6	
Density (calculated)	1.637 Mg/m^3	
Absorption coefficient	2.872 mm^{-1}	
F(000)	1848	
Crystal size	0.48 x 0.36 x 0.12 mm^3	
Theta range for data collection	2.742 to 68.193°.	
Index ranges	-10<=h<=9, -19<=k<=19, -31<=l<=31	
Reflections collected	66119	
Independent reflections	12961 [R(int) = 0.0513]	
Completeness to theta = 67.679°	96.7 %	
Absorption correction	Semi-empirical from equivalents	
Max. and min. transmission	0.7531 and 0.6805	
Refinement method	Full-matrix least-squares on F^2	
Data / restraints / parameters	12961 / 0 / 1069	
Goodness-of-fit on F^2	1.045	
Final R indices [I>2sigma(I)]	R_1 = 0.0400, wR_2 = 0.1087	
R indices (all data)	R_1 = 0.0467, wR_2 = 0.1125	
Extinction coefficient	n/a	
Largest diff. peak and hole	0.591 and -0.491 $e.Å^{-3}$	

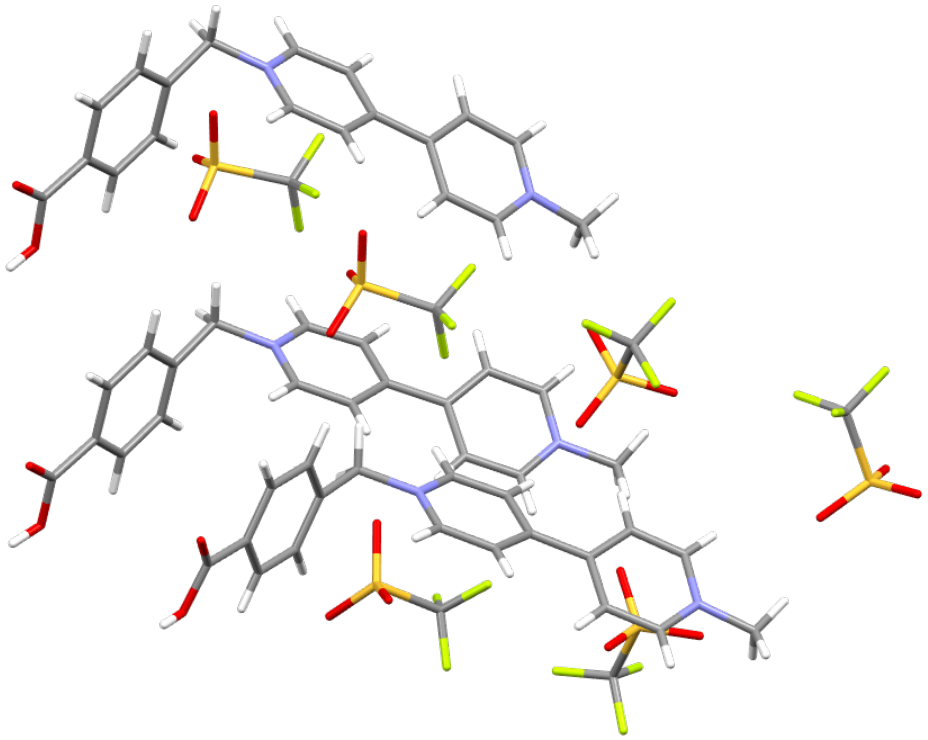

Figure S15. Molecular structure and packing of **MVA** in the solid state.

Table S3. Frontier Orbital energy levels based on DFT calculations performed at the B3LYP/6-31G(d) level of theory using the PCM solvation model.[S4]

	LUMO	HOMO	HOMO-1	Energy Gap
MVA	3.81	7.79	7.92	3.99
PVA	4.27	7.74	7.80	3.48
MVE	3.80	7.75	7.84	3.95
PVE	4.26	7.74	7.75	3.48

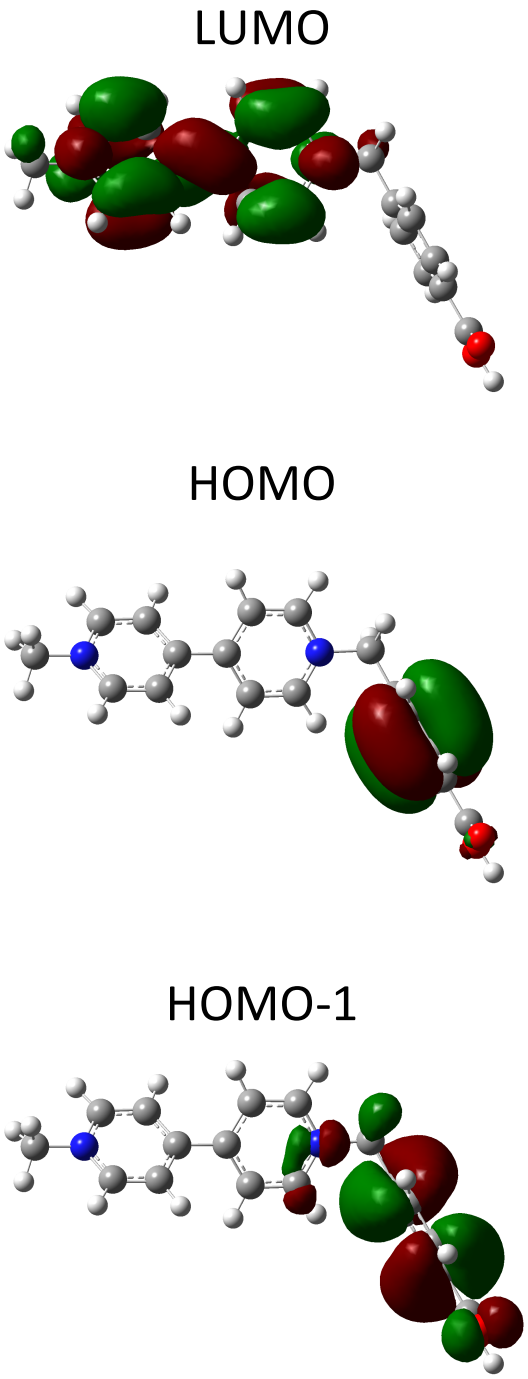

Figure S16. DFT calculations for **MVA**.

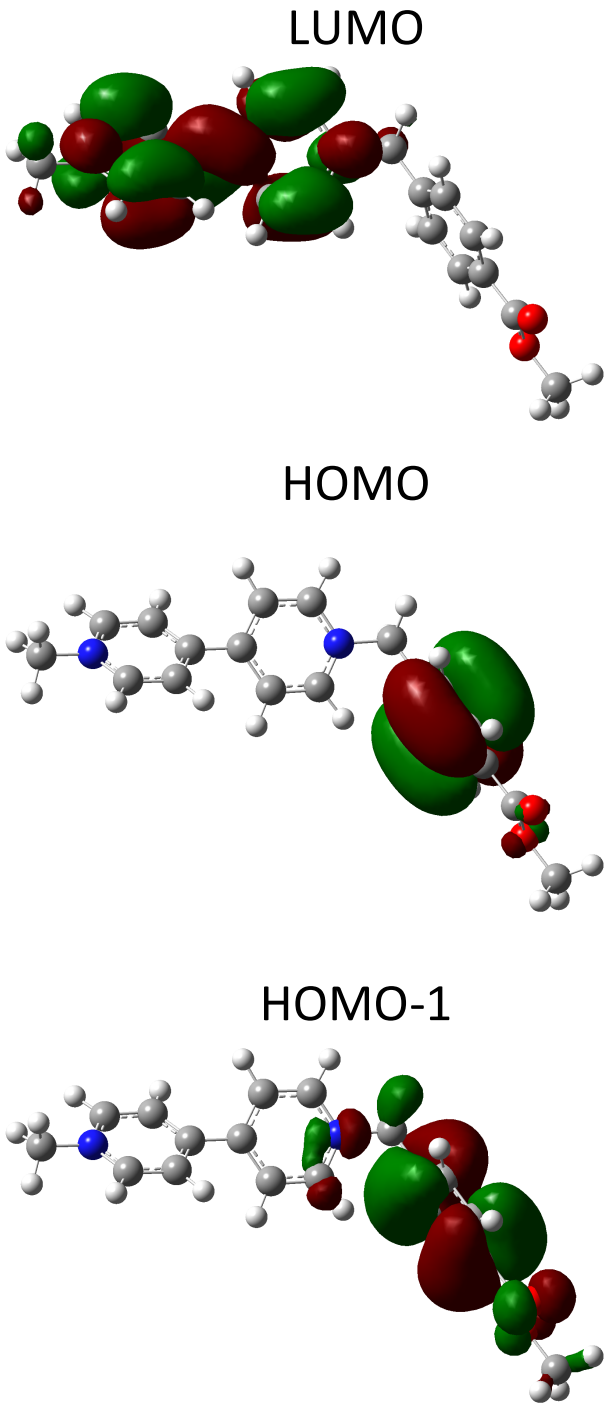

Figure S17. DFT calculations for **MVE**.

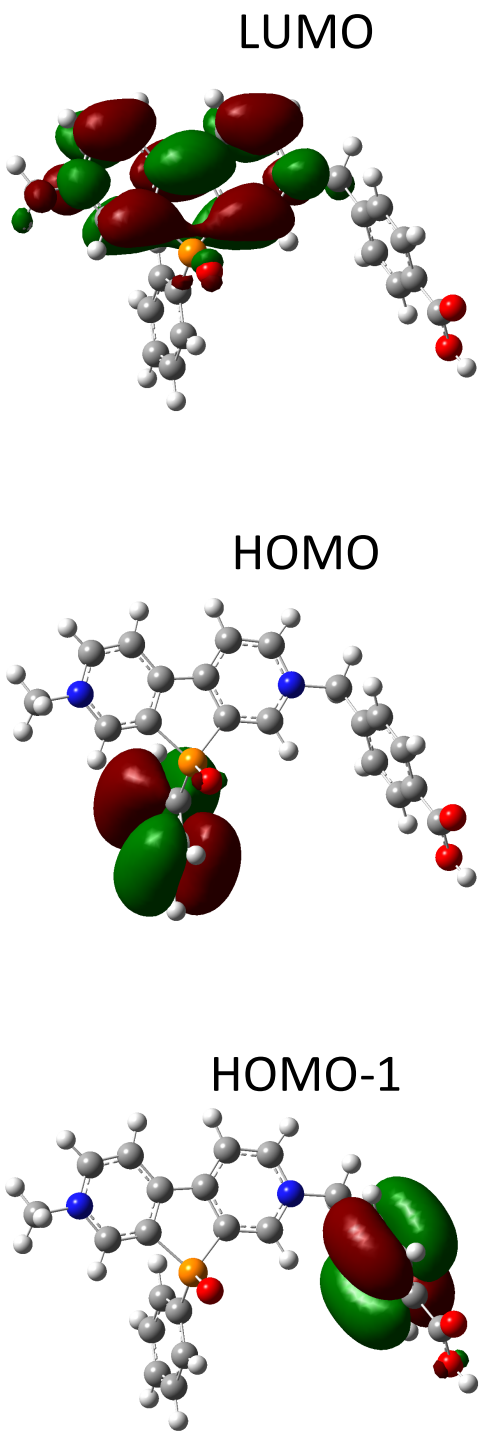

Figure S18. DFT calculations for **PVA**.

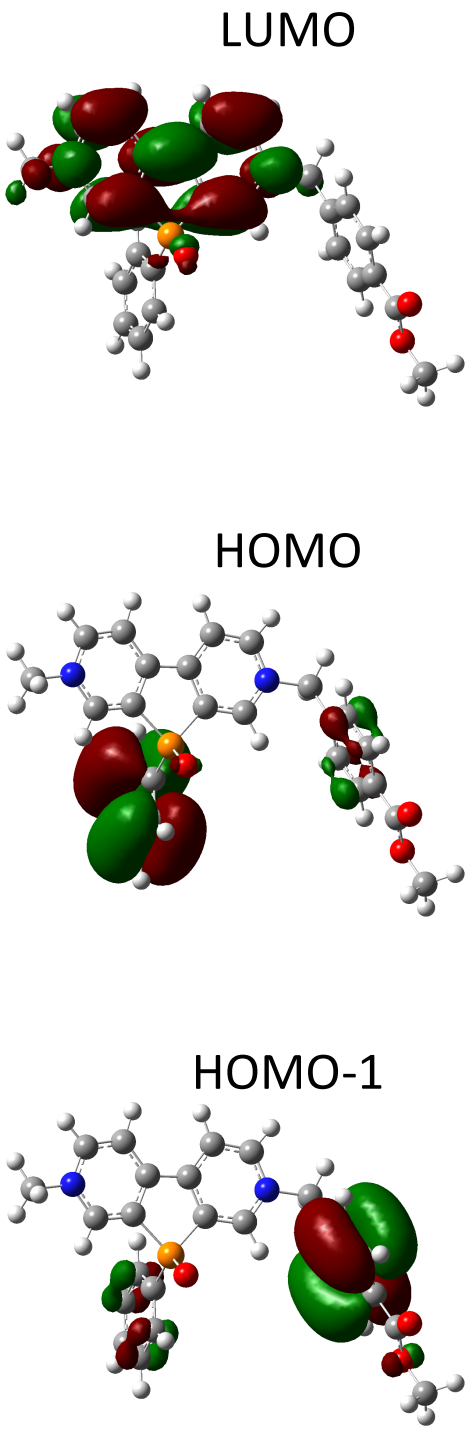

Figure S19. DFT calculations for **PVE**.

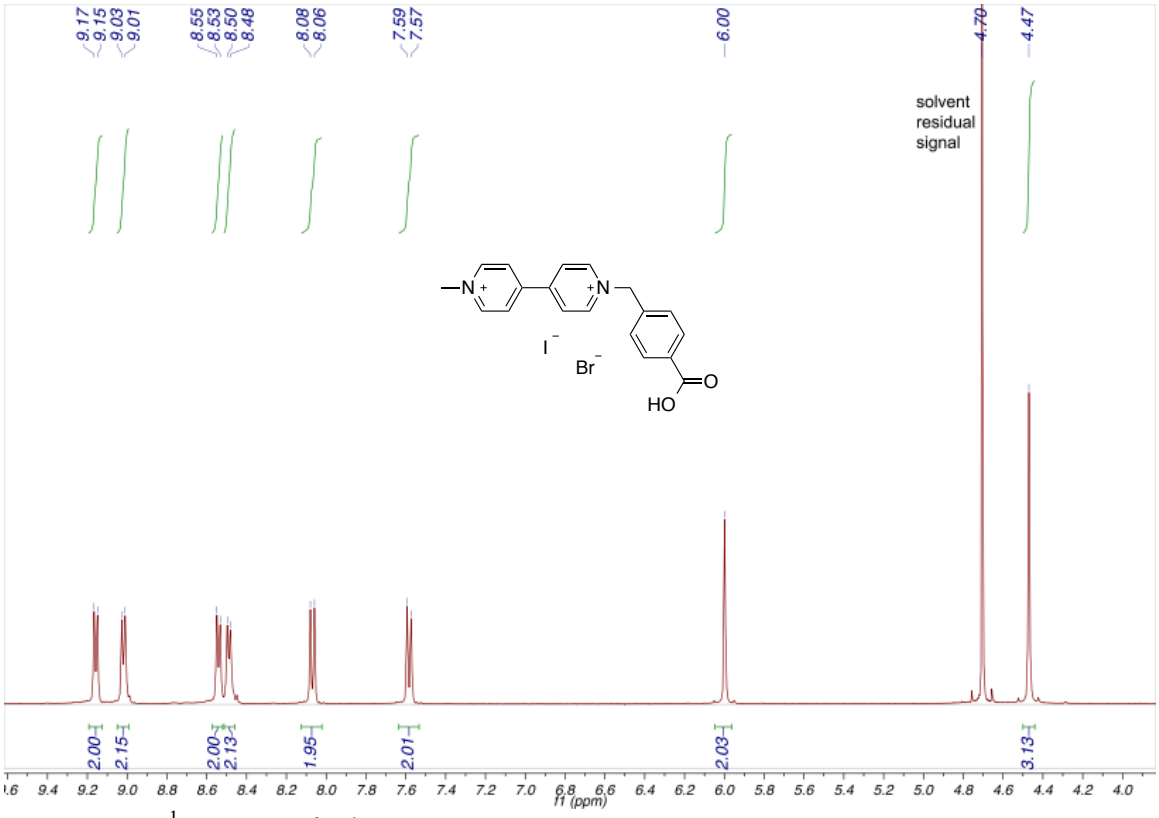

Figure S20. ^{1}H NMR of **2** in D_2O.

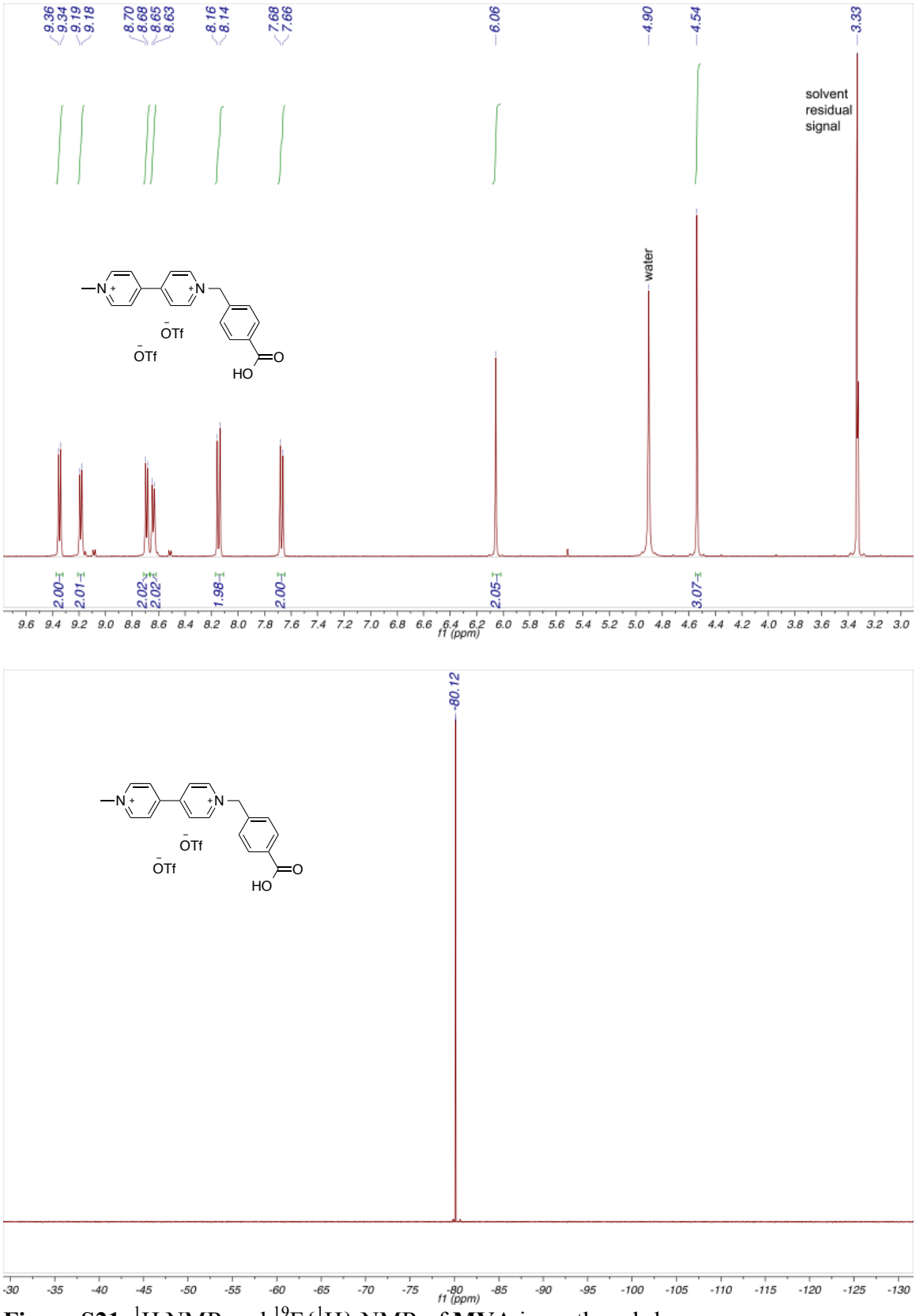

Figure S21. ^{1}H NMR and ^{19}F{^{1}H} NMR of **MVA** in methanol-d_4.

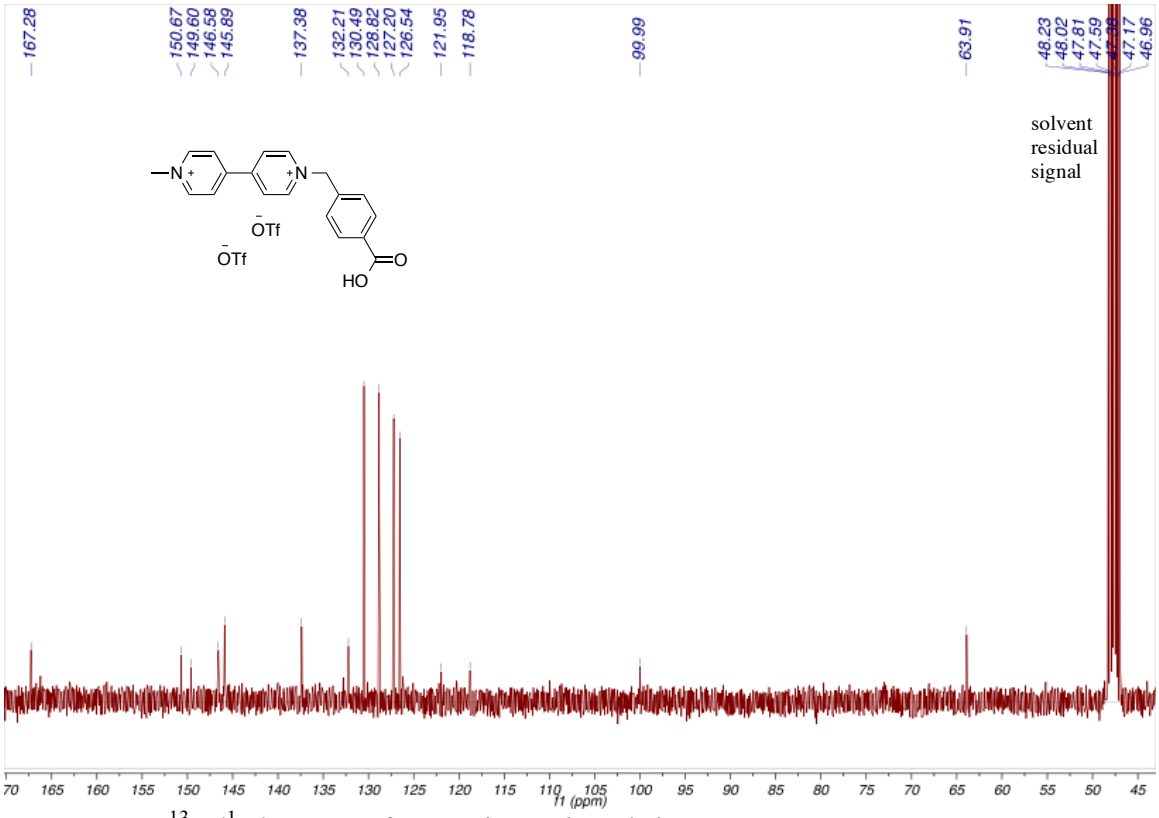

Figure S22. $^{13}C\{^{1}H\}$ NMR of **MVA** in methanol-d_4.

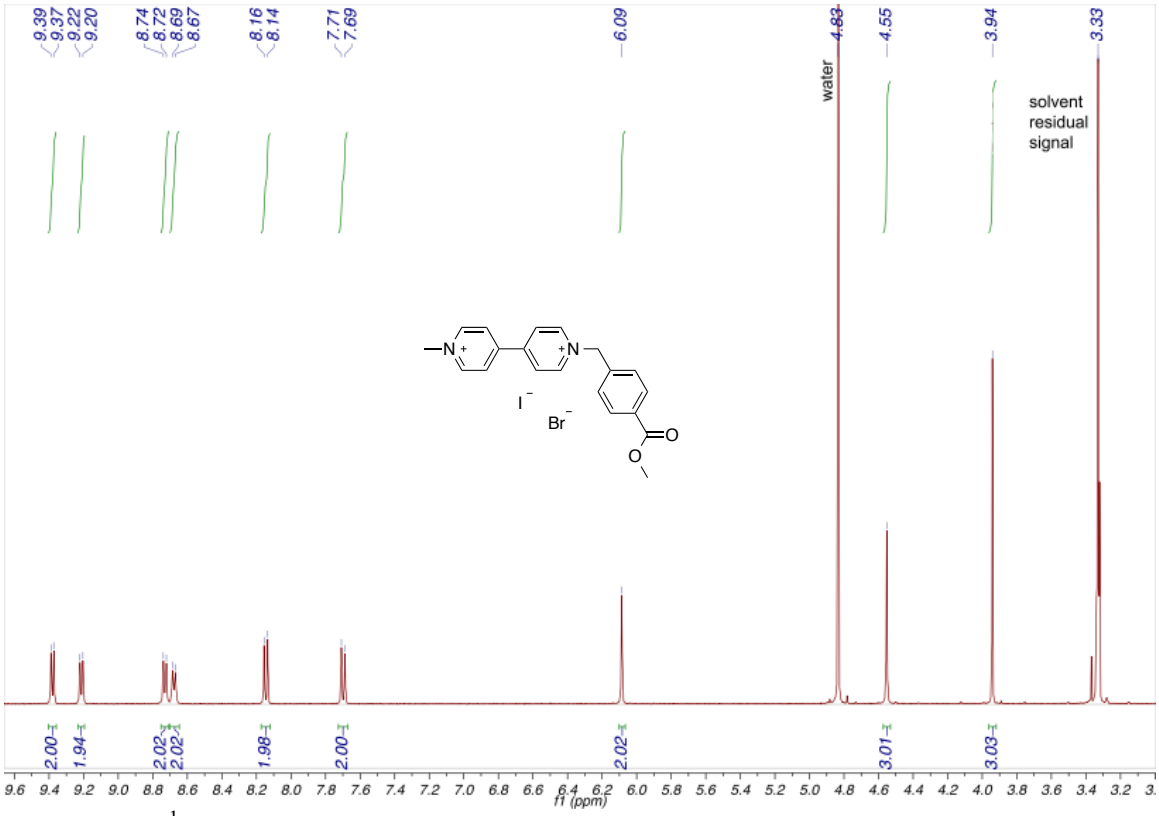

Figure S23. ^{1}H NMR of **3** in methanol-d_4.

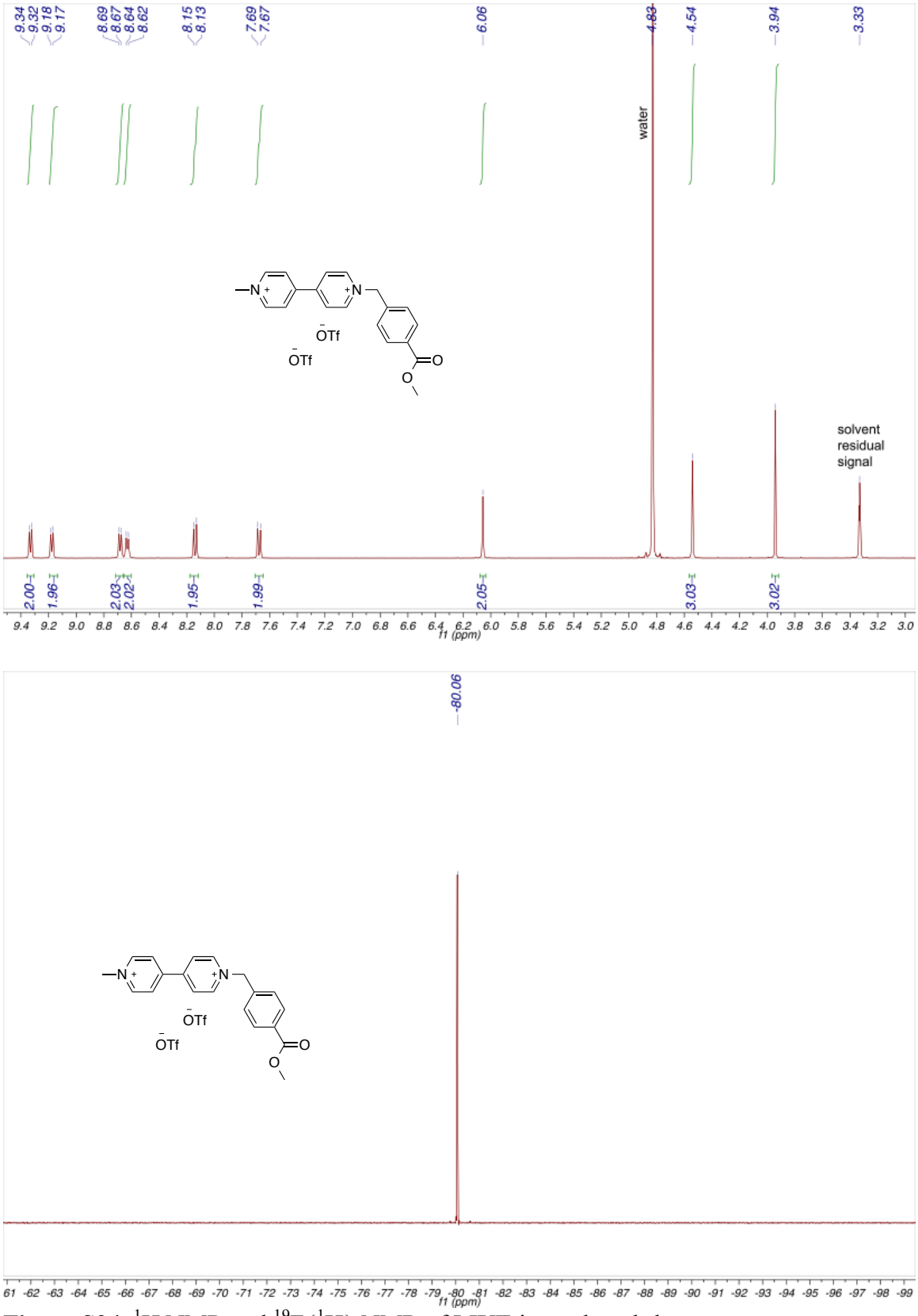

Figure S24. ^{1}H NMR and $^{19}F\{^{1}H\}$ NMR of **MVE** in methanol-d_4.

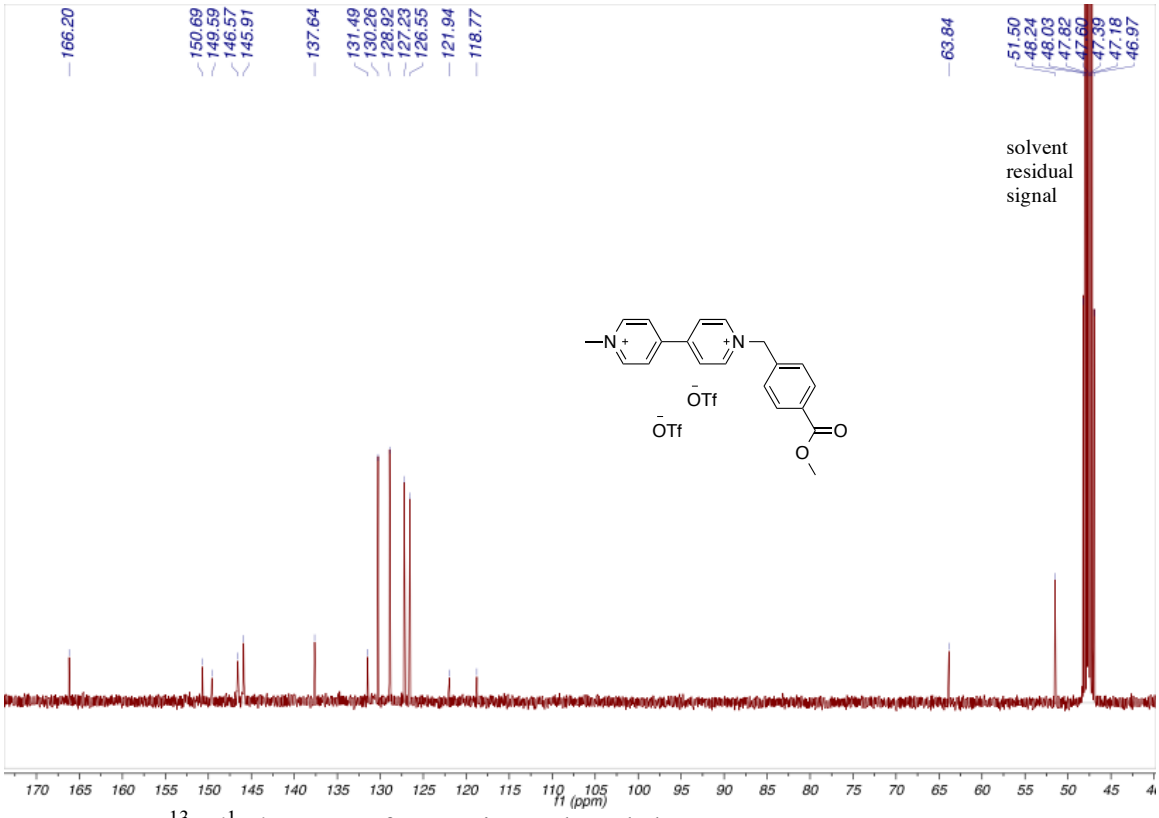

Figure S25. $^{13}C\{^{1}H\}$ NMR of **MVE** in methanol-d_4.

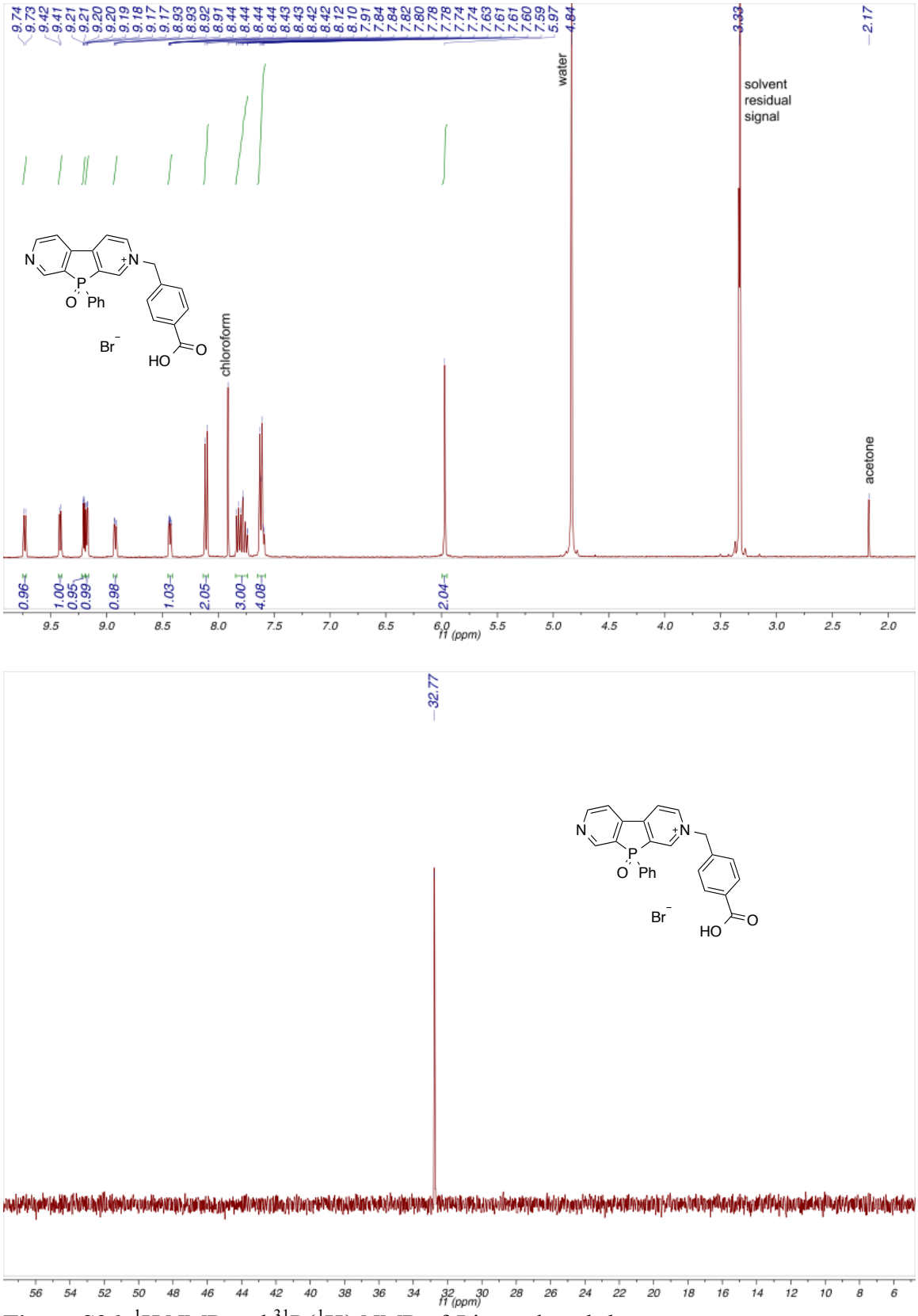

Figure S26. ^{1}H NMR and $^{31}P\{^{1}H\}$ NMR of **5** in methanol-d_4.

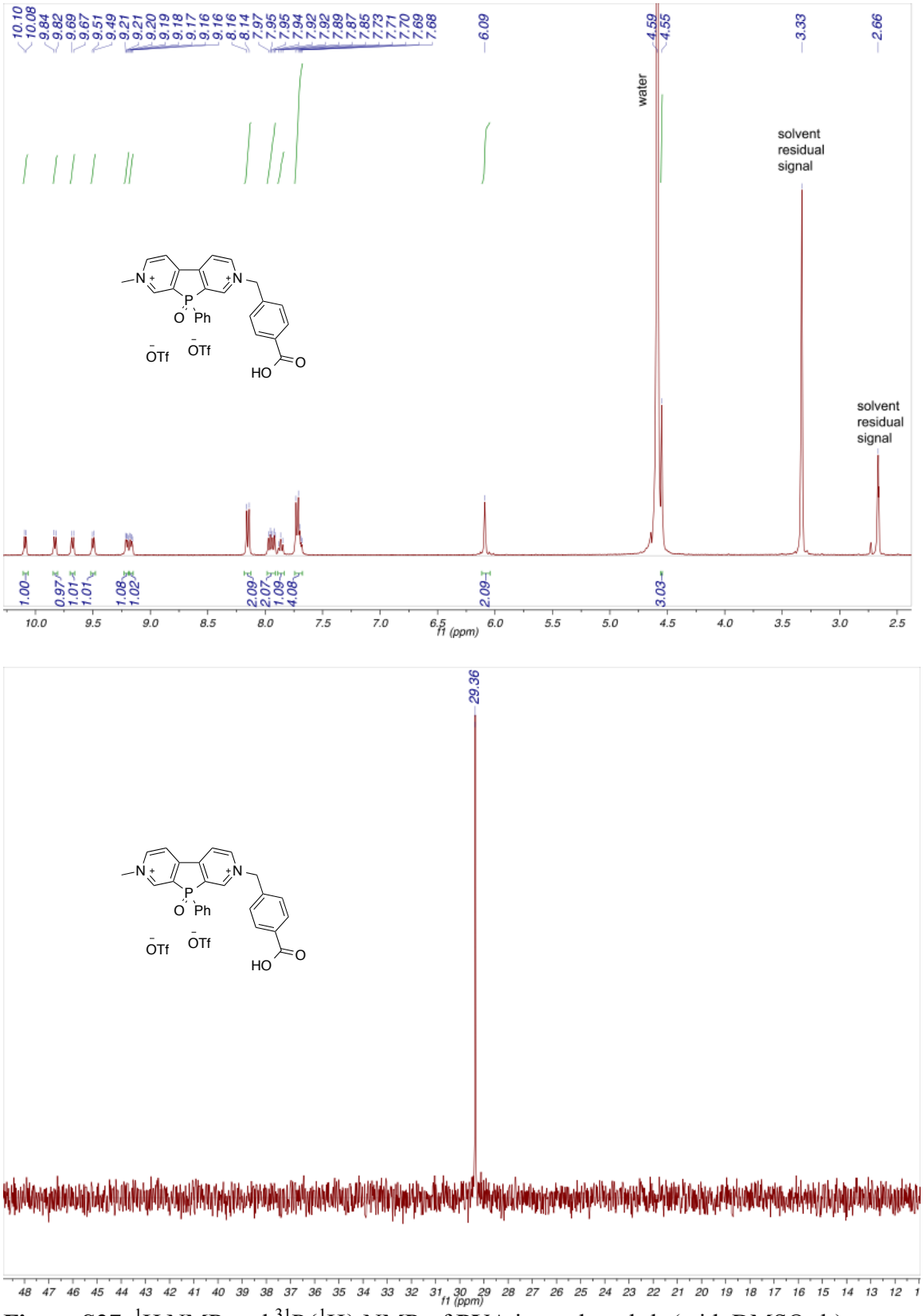

Figure S27. ^{1}H NMR and ^{31}P{^{1}H} NMR of **PVA** in methanol-d_4 (with DMSO-d_6).

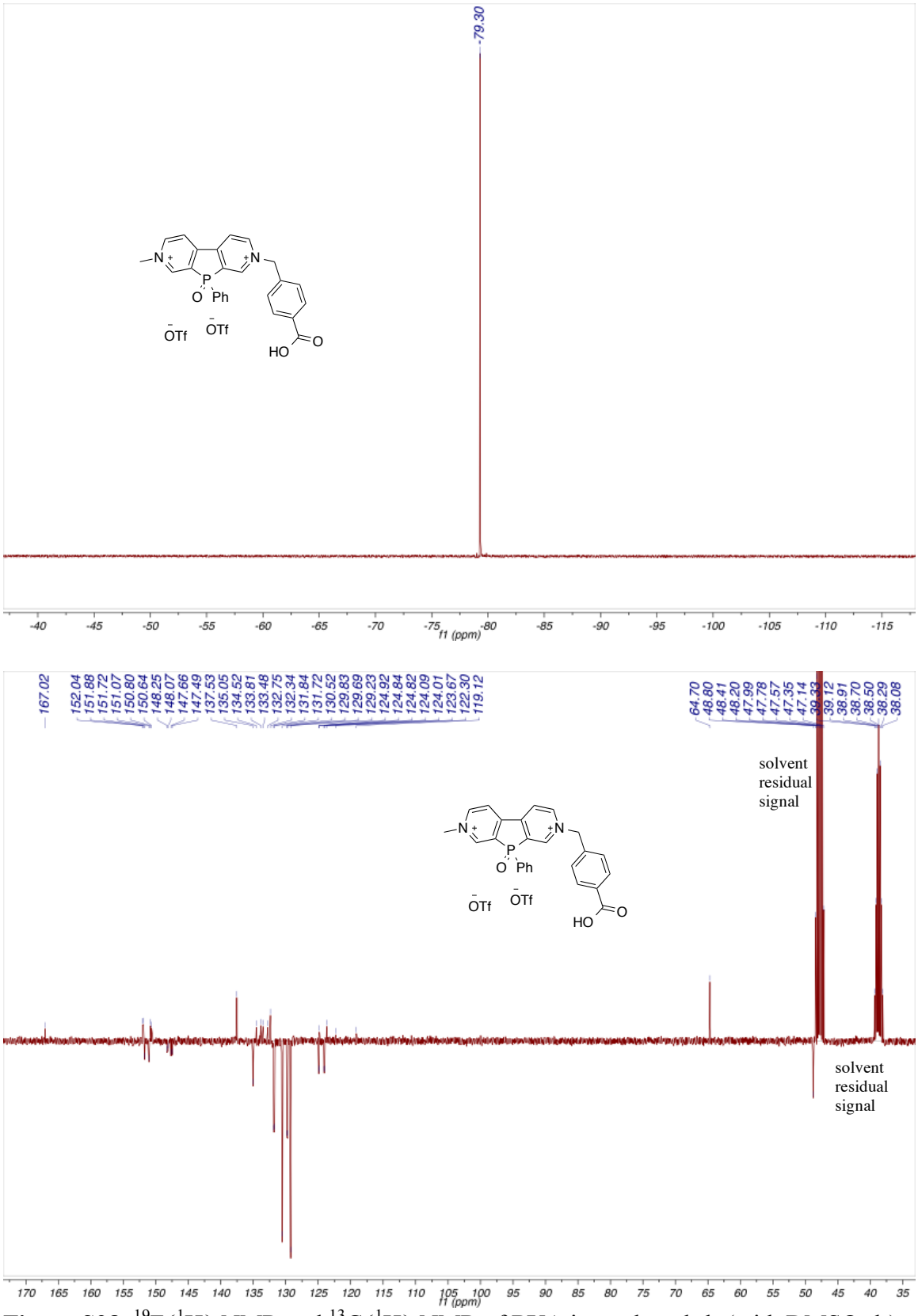

Figure S28. $^{19}F\{^{1}H\}$ NMR and $^{13}C\{^{1}H\}$ NMR of **PVA** in methanol-d_4 (with DMSO-d_6).

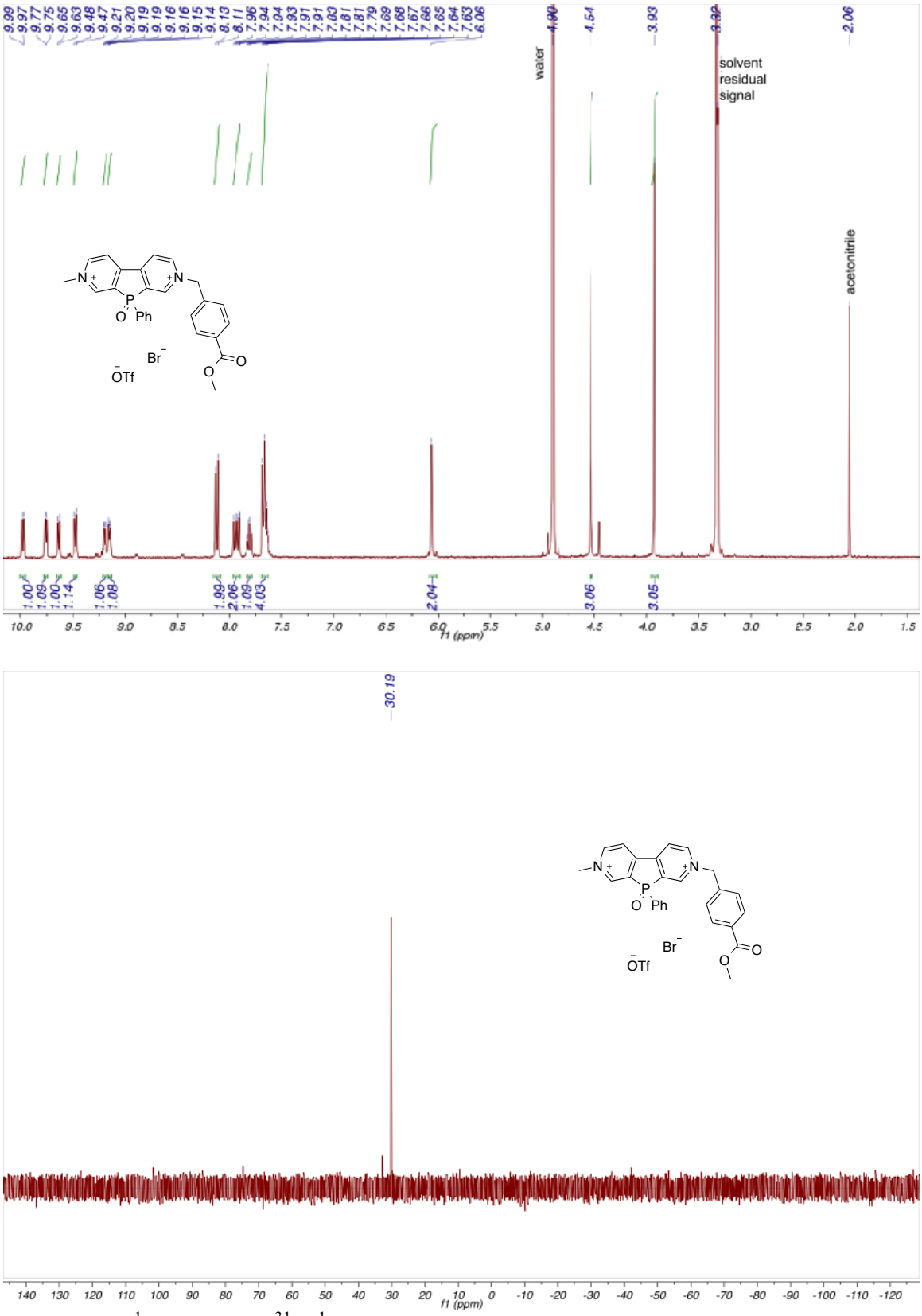

Figure S29. ^{1}H NMR and $^{31}P\{^{1}H\}$ NMR of **7** in methanol-d_4.

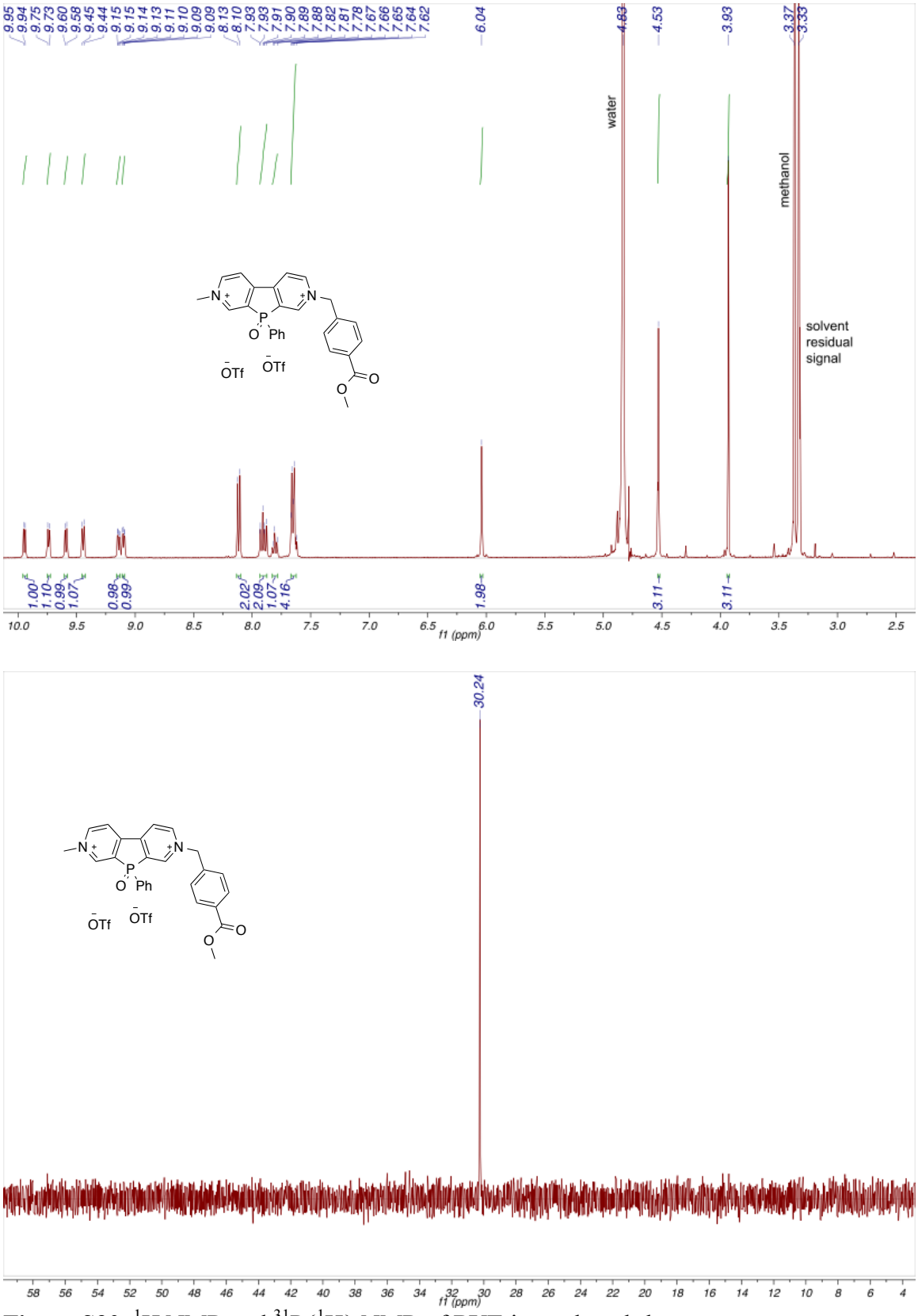

Figure S30. ^{1}H NMR and $^{31}P\{^{1}H\}$ NMR of **PVE** in methanol-d_4.

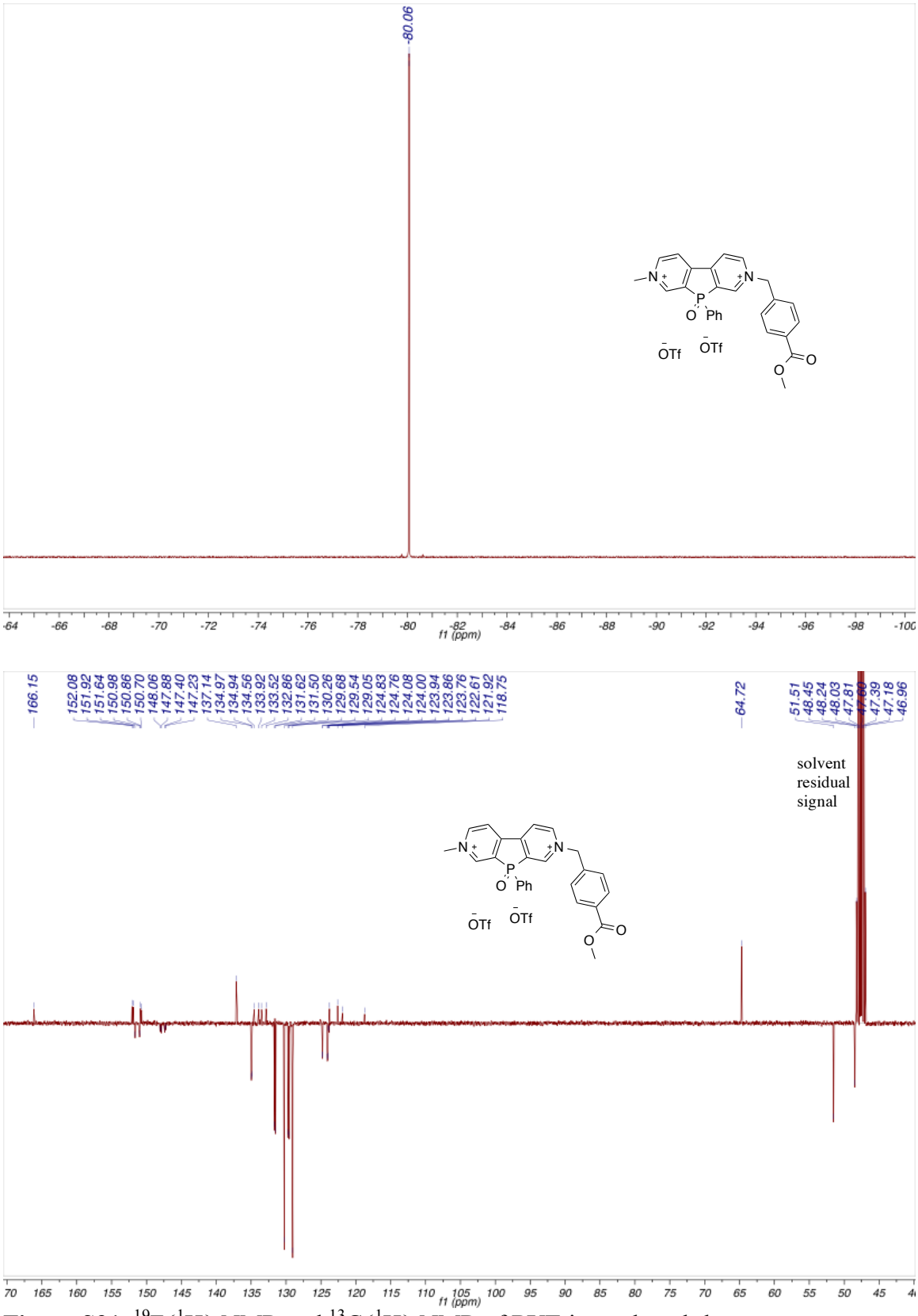

Figure S31. $^{19}F\{^{1}H\}$ NMR and $^{13}C\{^{1}H\}$ NMR of **PVE** in methanol-d_4.

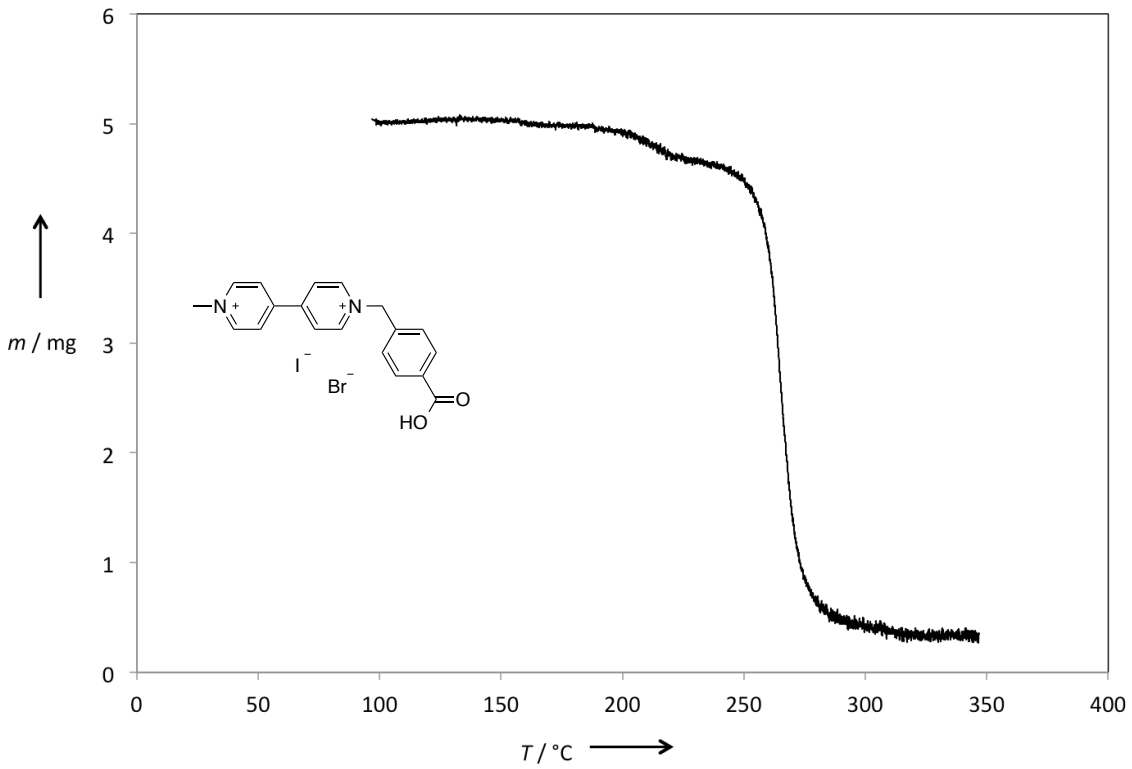

Figure S32. TGA of **2**.

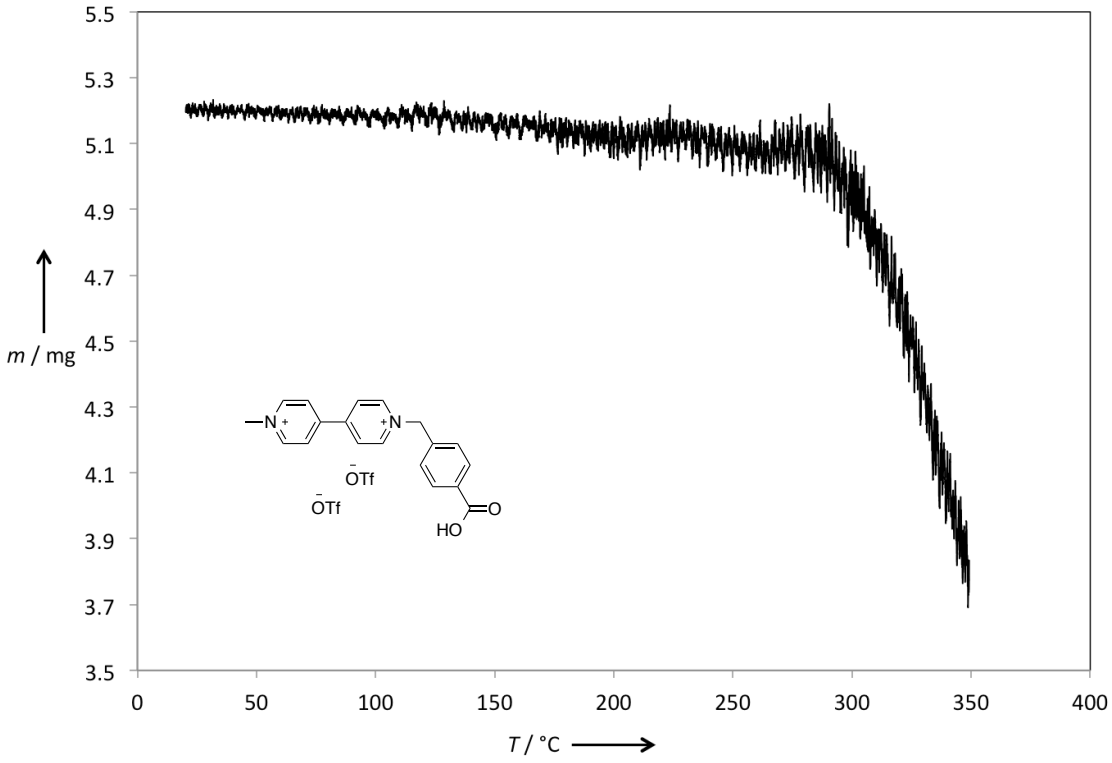

Figure S33. TGA of **MVA**.

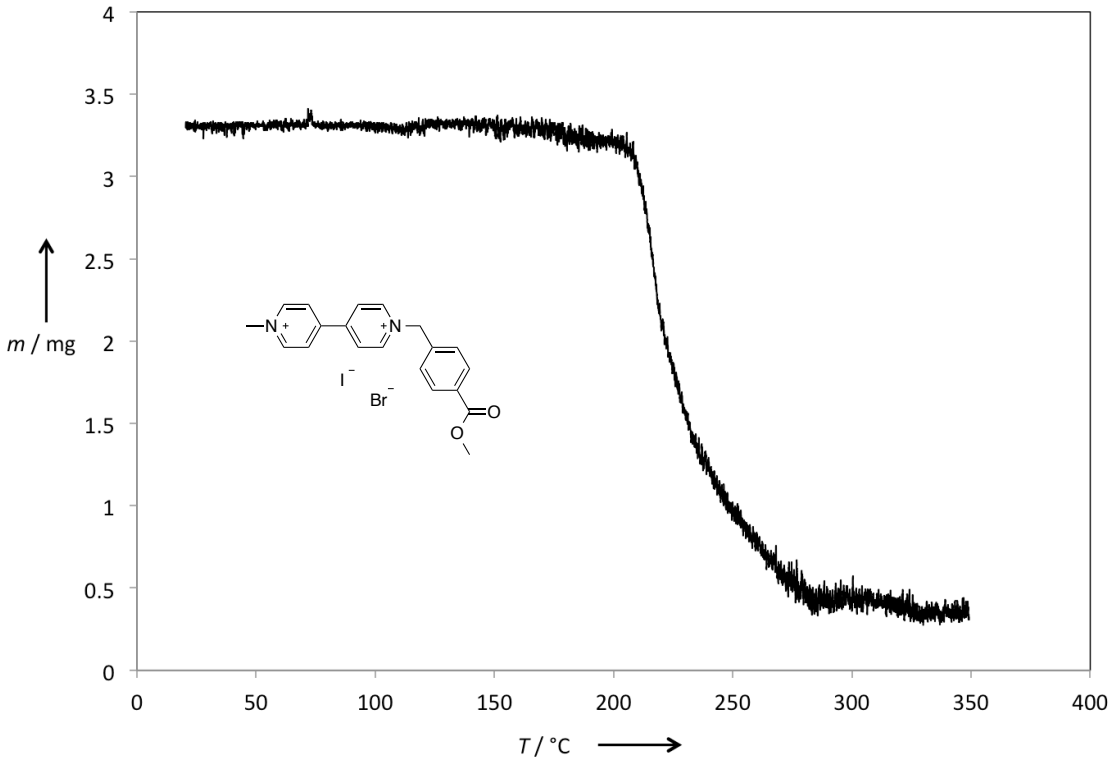

Figure S34. TGA of **3**.

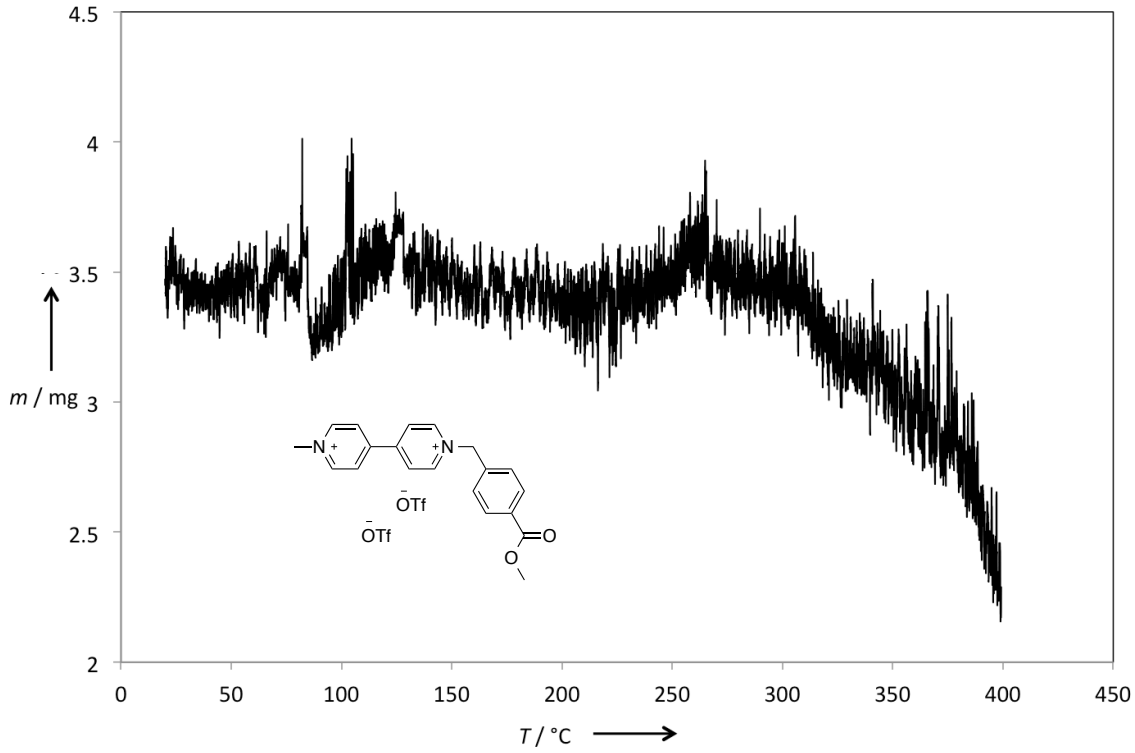

Figure S35. TGA of **MVE**.

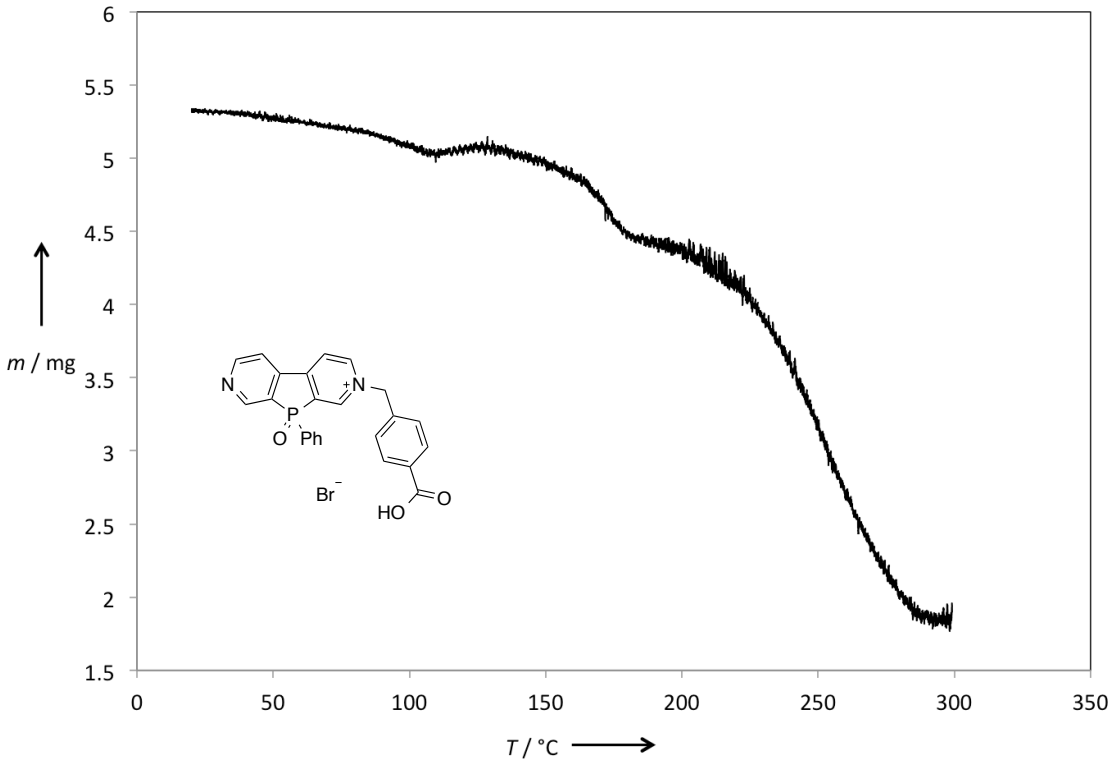

Figure S36. TGA of **5**.

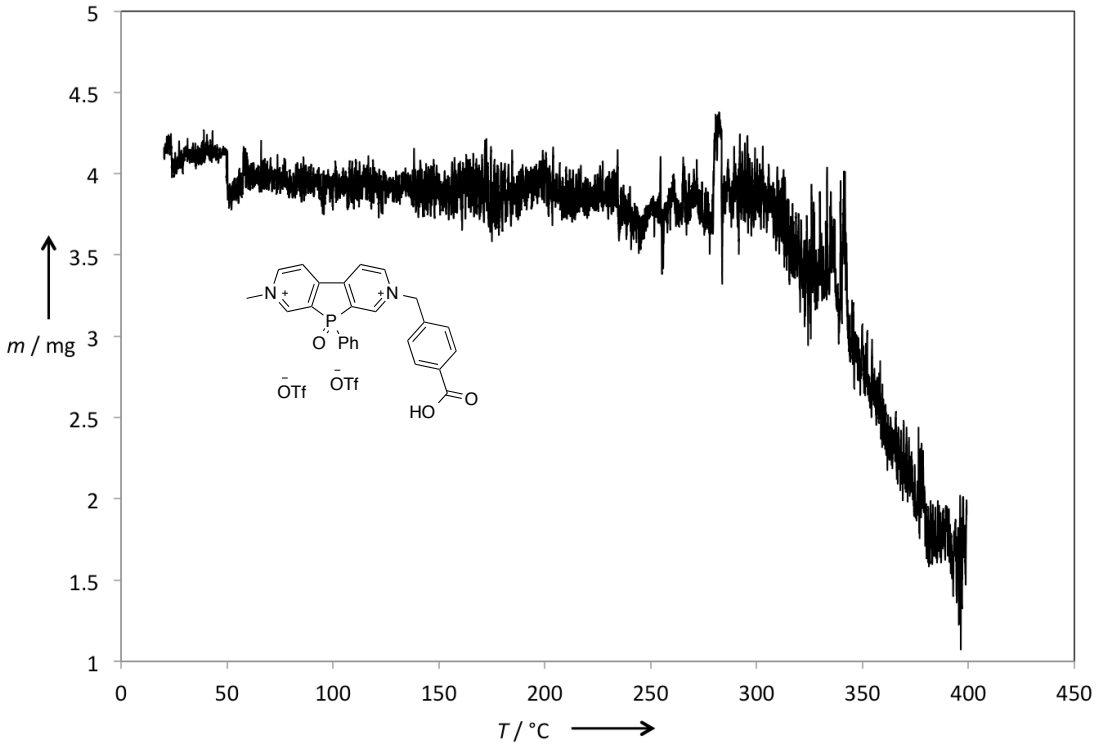

Figure S37. TGA of **PVA**.

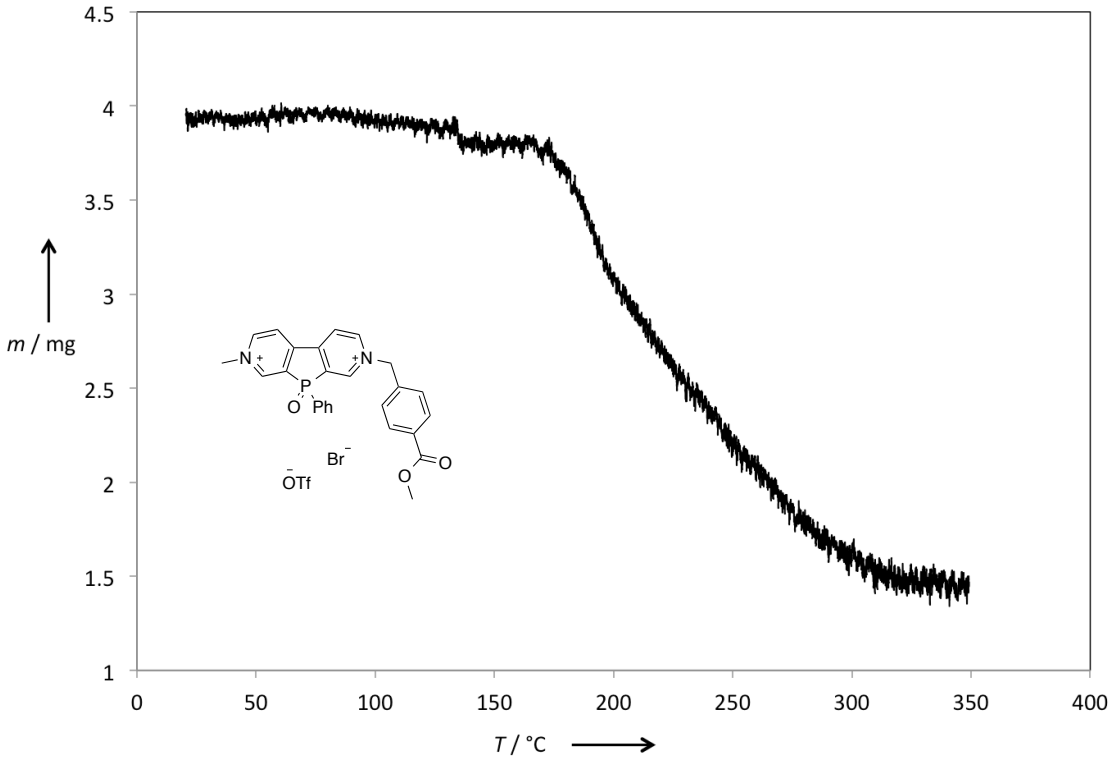

Figure S38. TGA of **7**.

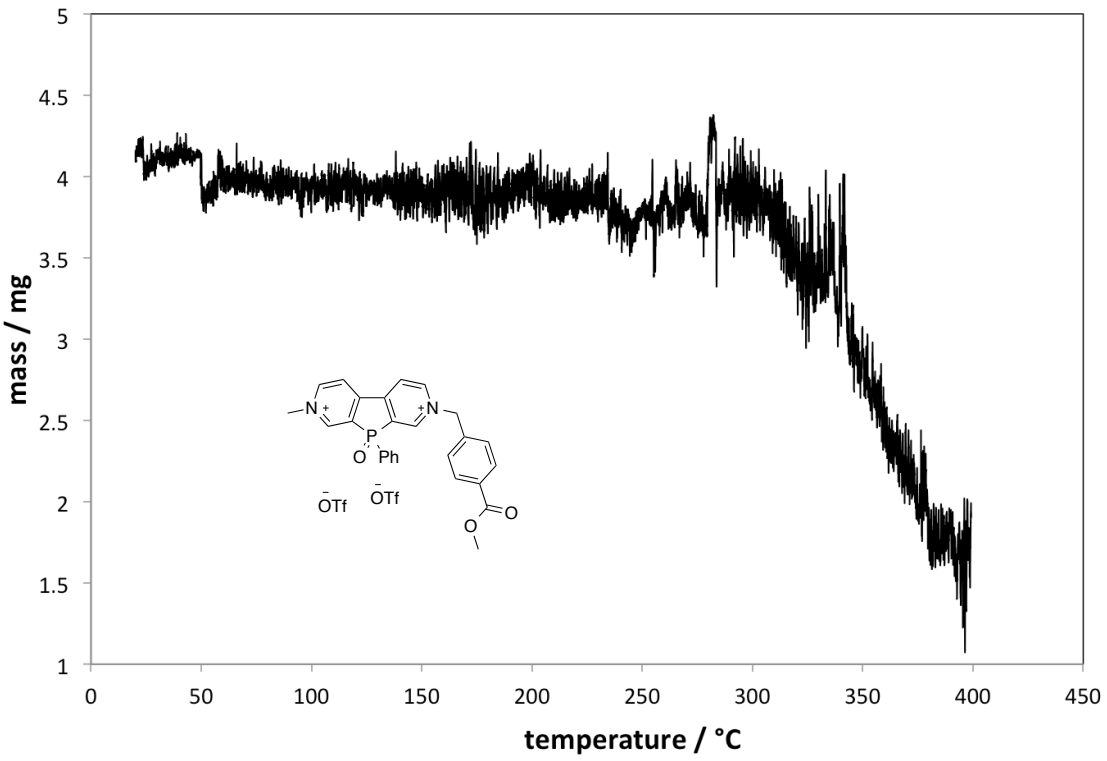

Figure S39. TGA of **PVE**.

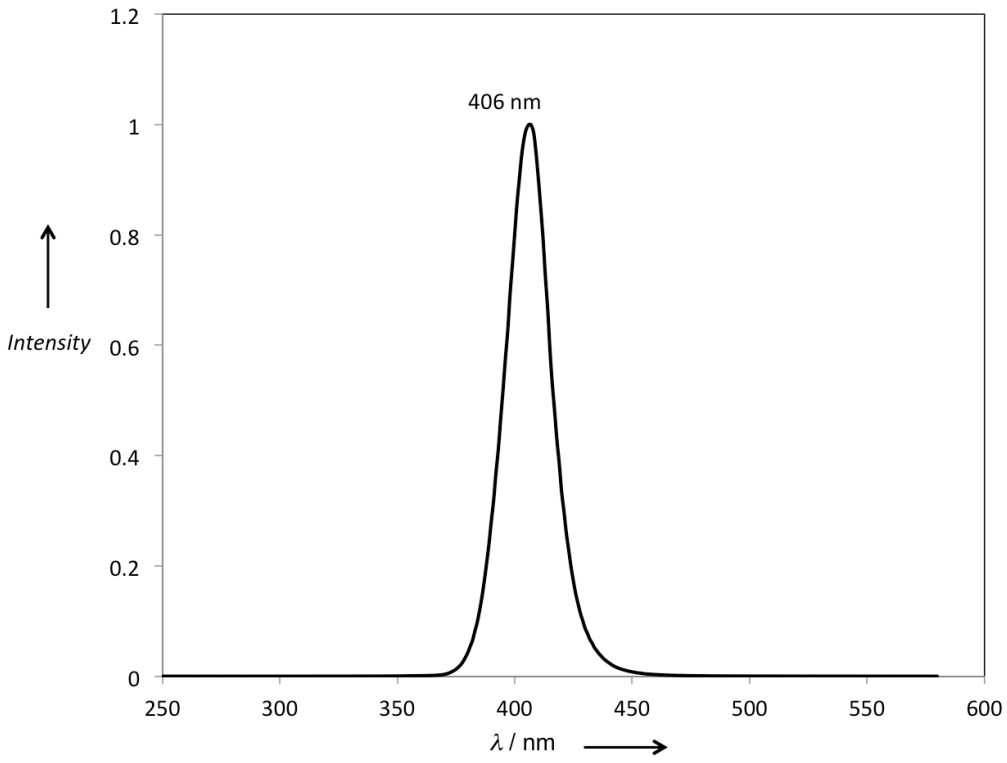

Figure S40. Spectral profile of 2W LED purchased from Lumex.

References

[S1] E. L. Robb, J. M. Gawel, D. Aksentijević, H. M. Cochemé, T. S. Stewart, M. M. Shchepinova, H. Qiang, T. A. Prime, T. P. Bright, A. M. James, M. J. Shattock, H. M. Senn, R. C. Hartley, M. P. Murphy, *Free Radical Biology and Medicine,* **2015**, *89,* 883–894.

[S2] S. Durben, T. Baumgartner, *Angew. Chem.* **2011**, *123*, 8096-8100; *Angew. Chem. Int. Ed.* **2011**, *50*, 7948-7952.

[S3] M. Stolar, C. Reus, T. Baumgartner, *Adv. Energy Mater.* **2016**, *6*, 1600944.

[S4] M. J. Frisch, G. W. Trucks, H. B. Schlegel, G. E. Scuseria, M. A. Robb, J. R. Cheeseman, J. A. Montgomery, Jr., T. Vreven, K. N. Kudin, J. C. Burant, J. M. Millam, S. S. Iyengar, J. Tomasi, V. Barone, B. Mennucci, M. Cossi, G. Scalmani, N. Rega, G. A. Petersson, H. Nakatsuji, M. Hada, M. Ehara, K. Toyota, R. Fukuda, J. Hasegawa, M. Ishida, T. Nakajima, Y. Honda, O. Kitao, H. Nakai, M. Klene, X. Li, J. E. Knox, H. P. Hratchian, J. B. Cross, V. Bakken, C. Adamo, J. Jaramillo, R. Gomperts, R. E. Stratmann, O. Yazyev, A. J. Austin, R. Cammi, C. Pomelli, J. W. Ochterski, P. Y. Ayala, K. Morokuma, G. A. Voth, P. Salvador, J. J. Dannenberg, V. G. Zakrzewski, S. Dapprich, A. D. Daniels, M. C. Strain, O. Farkas, D. K. Malick, A. D. Rabuck, K. Raghavachari, J. B. Foresman, J. V. Ortiz, Q. Cui, A. G. Baboul, S. Clifford, J. Cioslowski, B. B. Stefanov, G. Liu, A. Liashenko, P. Piskorz, I. Komaromi, R. L. Martin, D. J. Fox, T. Keith, M. A. Al-Laham, C. Y. Peng, A. Nanayakkara, M. Challacombe, P. M. W. Gill, B. Johnson, W. Chen, M.W. Wong, C. Gonzalez, J. A. Pople, Gaussian Inc., Wallingford, CT, 2007.